# Finite-frequency body-wave tomography on a global scale

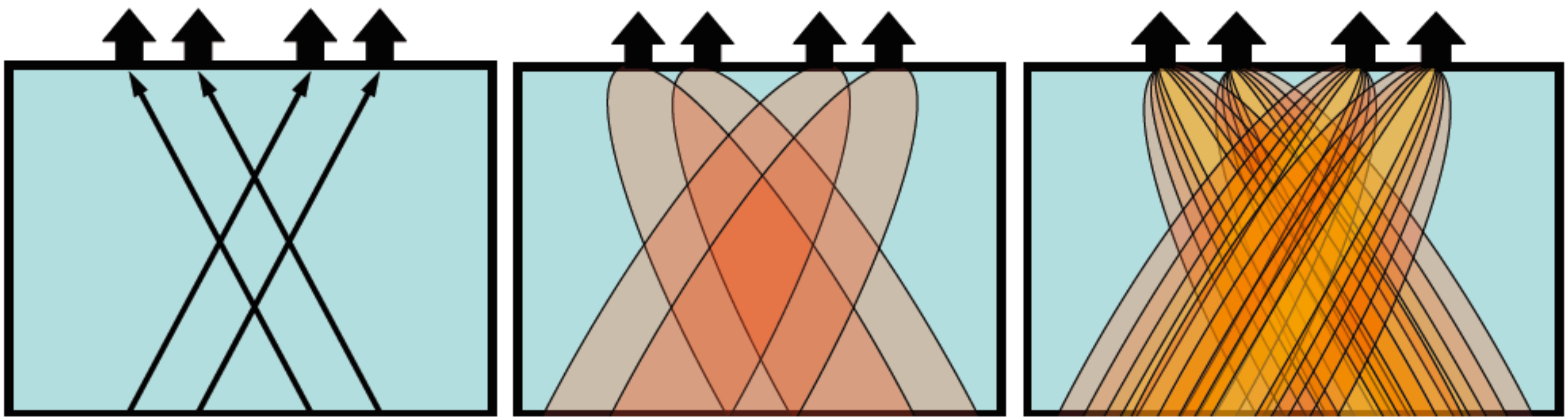

Karin Sigloch

Ludwig-Maximilians-Universität Munich

# Broadband seismograms, the raw material for waveform-based tomography

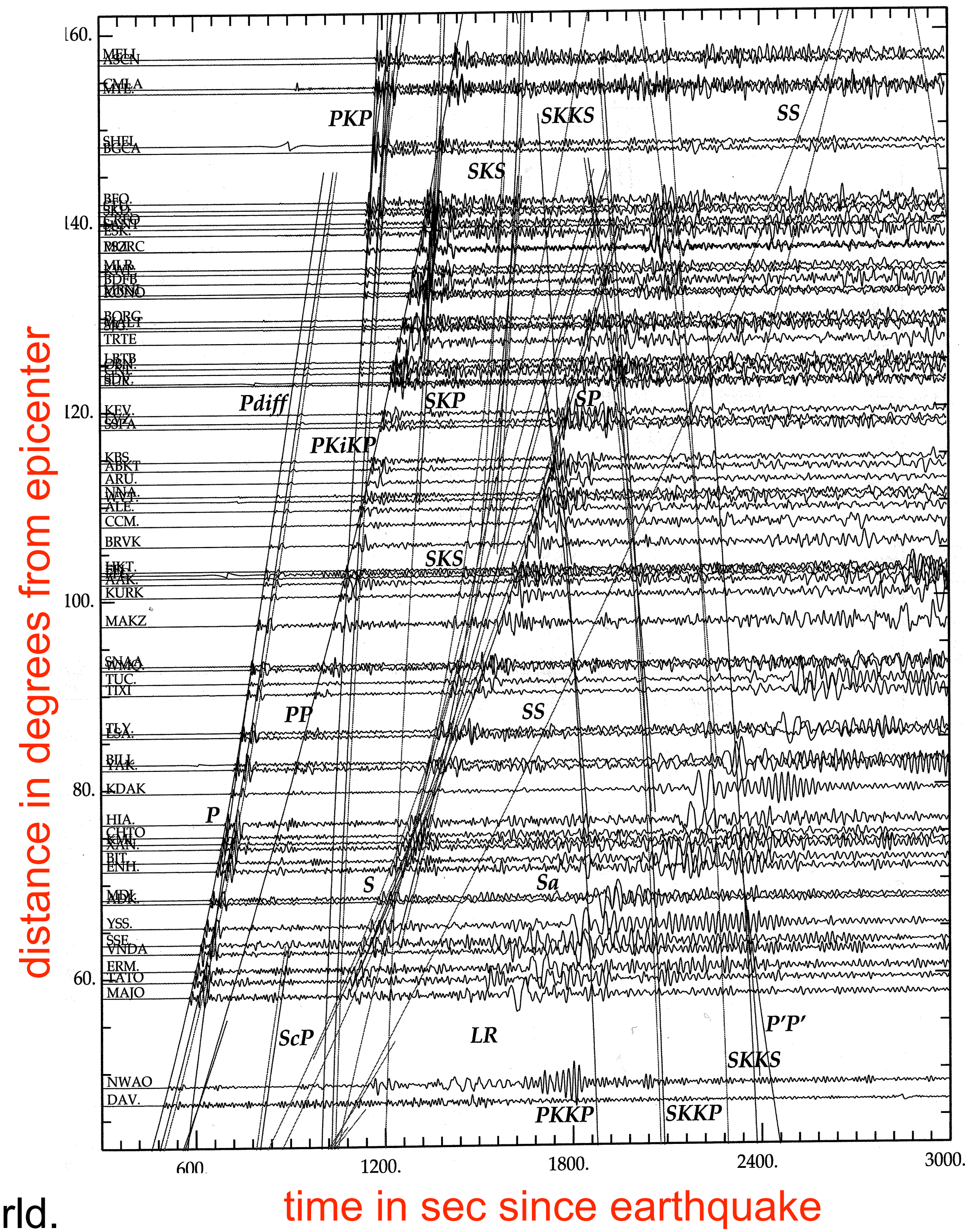


A earthquake of magnitude 6.8 in Vanuatu, recorded around the world.

…parts presently used (or targeted) for finite-frequency inversion

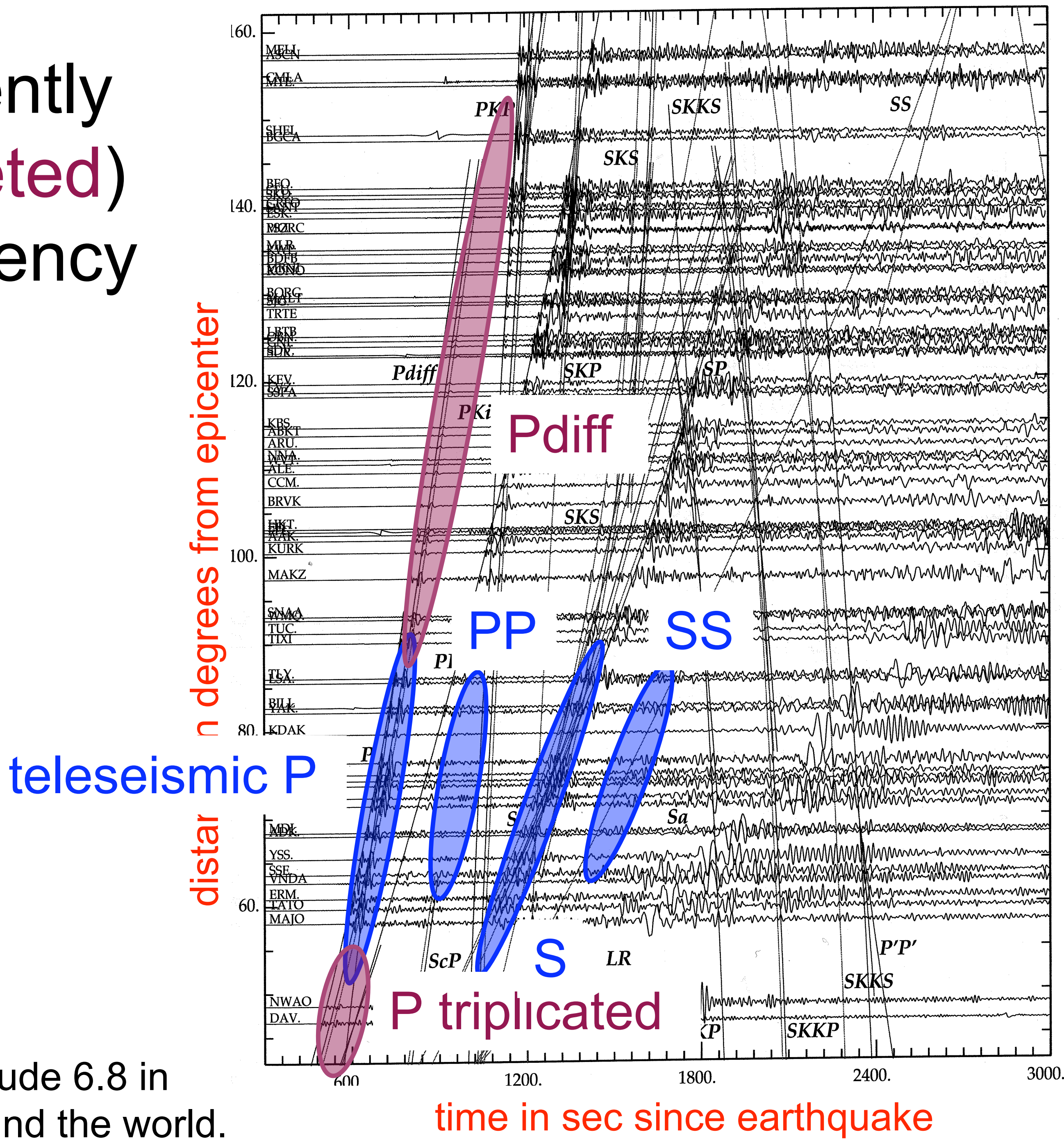


A earthquake of magnitude 6.8 in Vanuatu, recorded around the world.

# Finite-frequency measurements

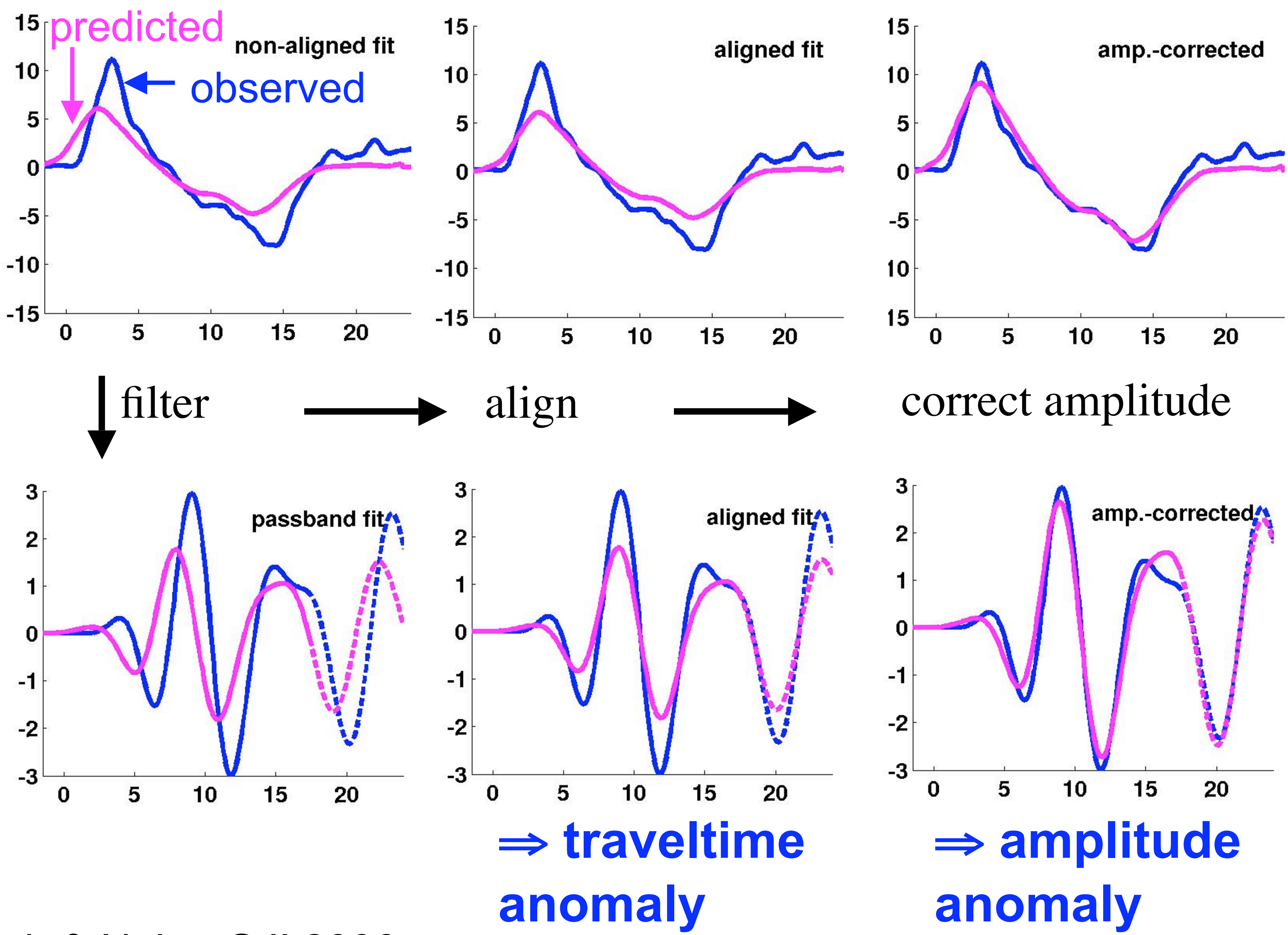


Sigloch & Nolet, GJI 2006

# Passband filters

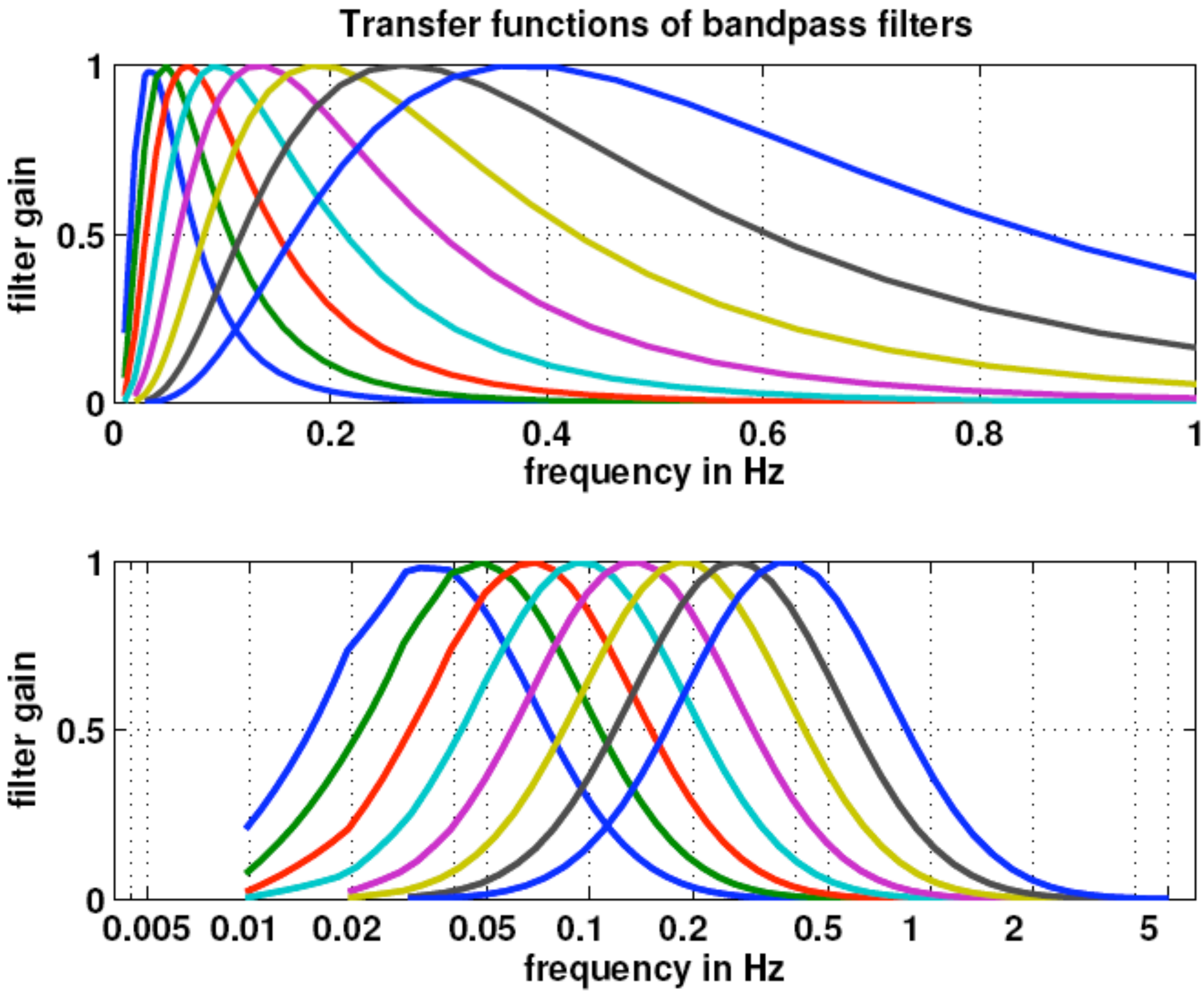

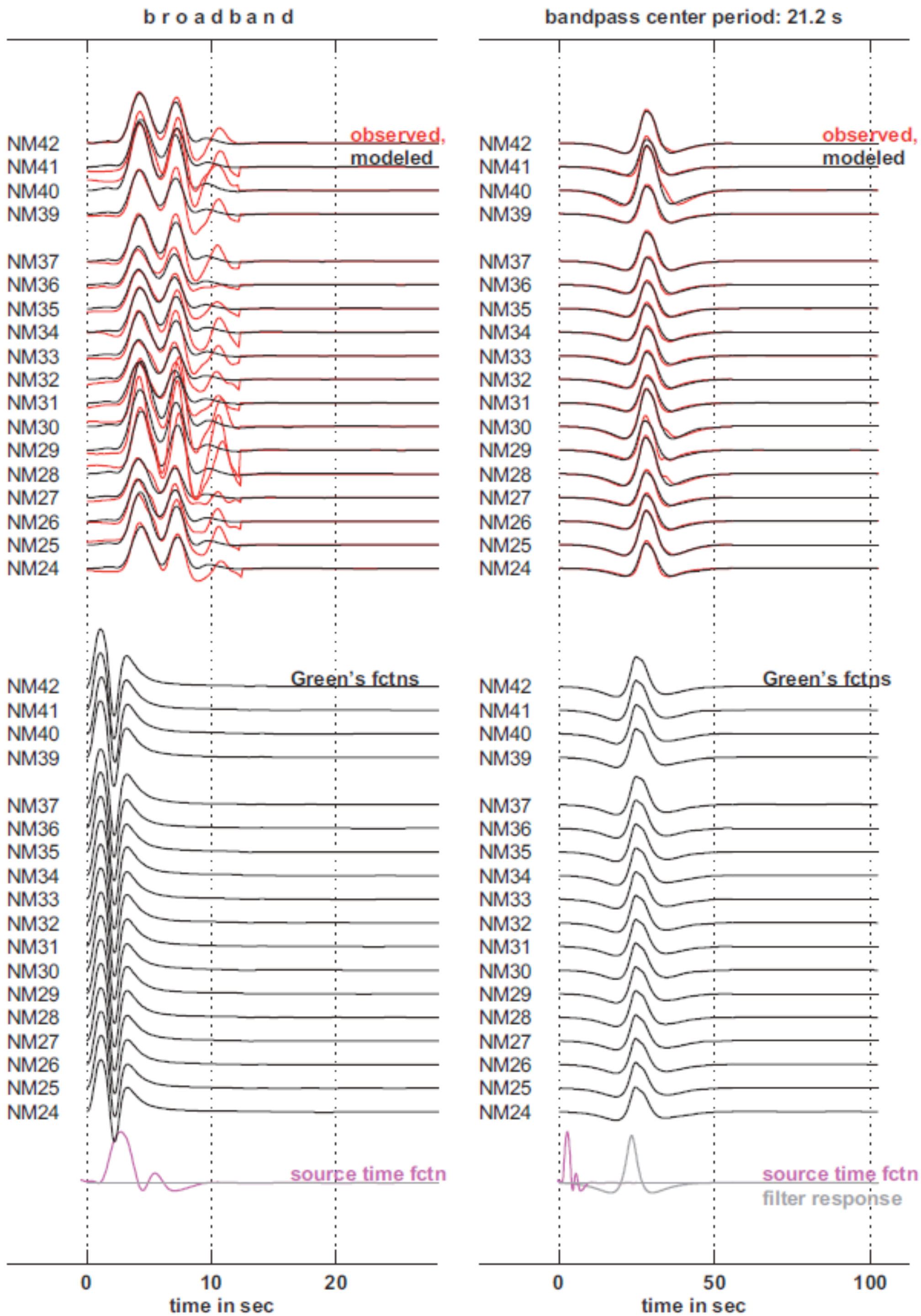


# Generating data: observed waveforms and their matched filters

Left: broadband seismograms

Right: bandpassed to 21 s dominant period

# Generating data: observed waveforms and their matched filters

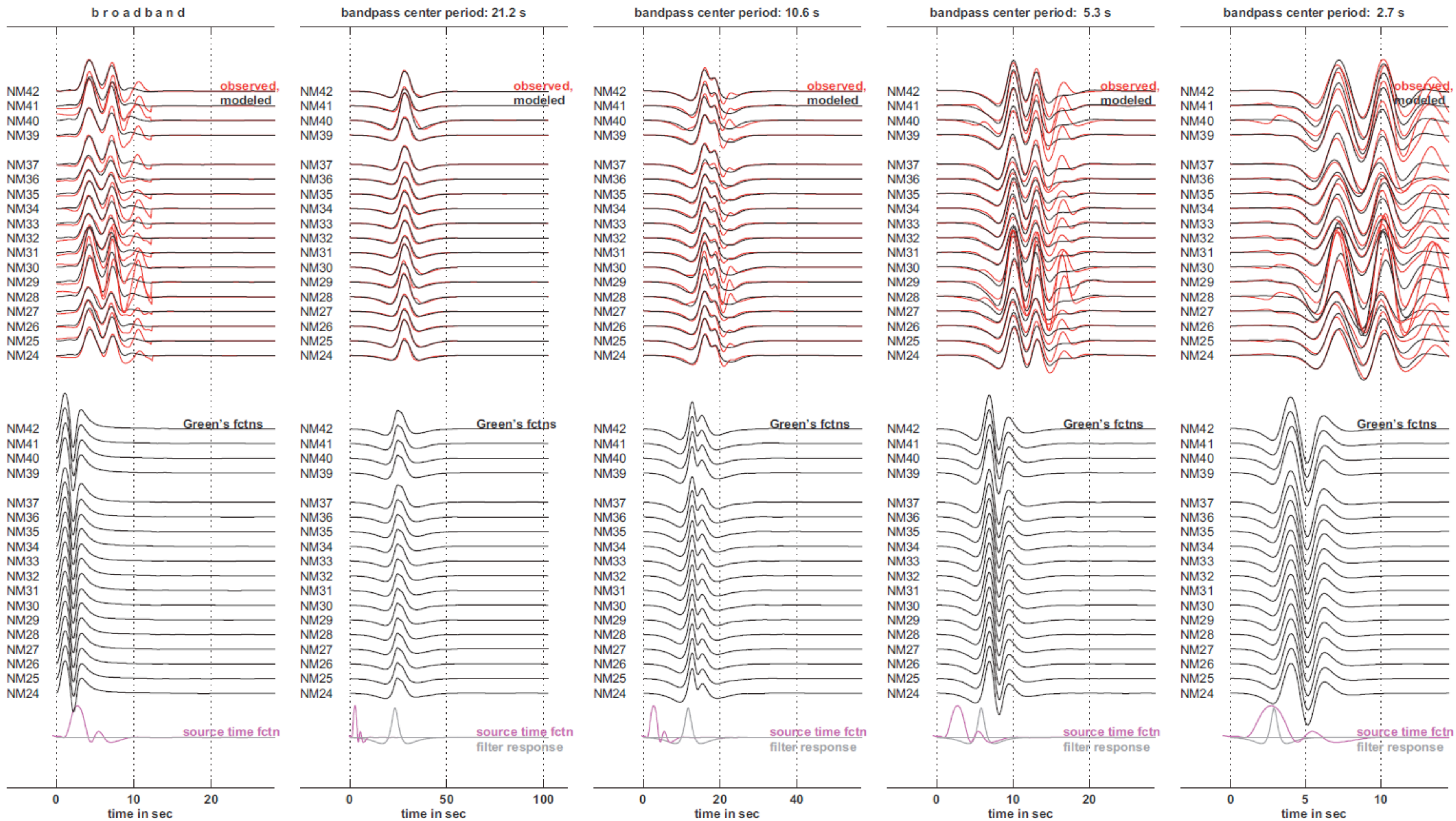

# Finite-frequency data for tomography

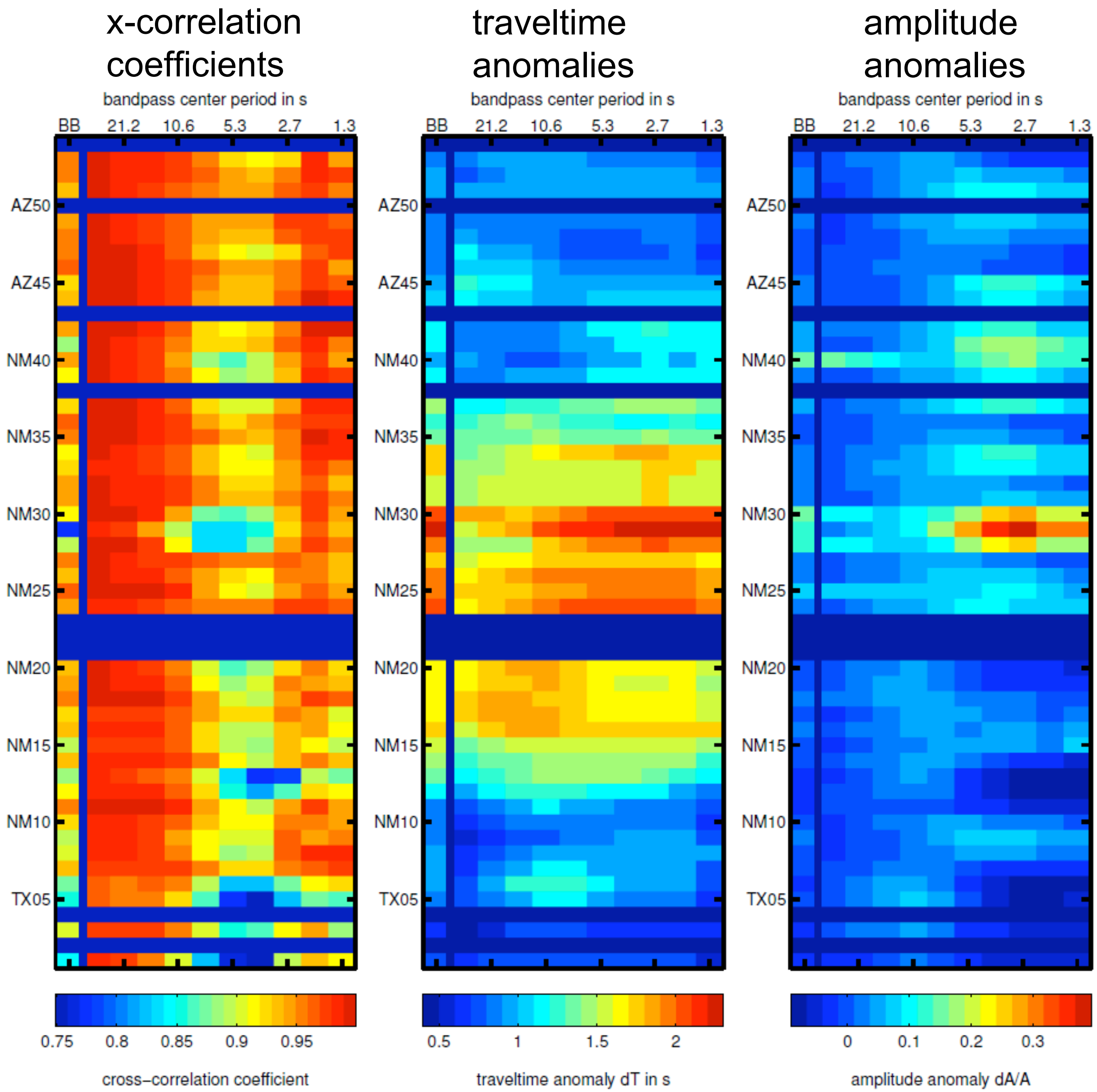

# Frequency-dependent measurements multiply the constraints on structure

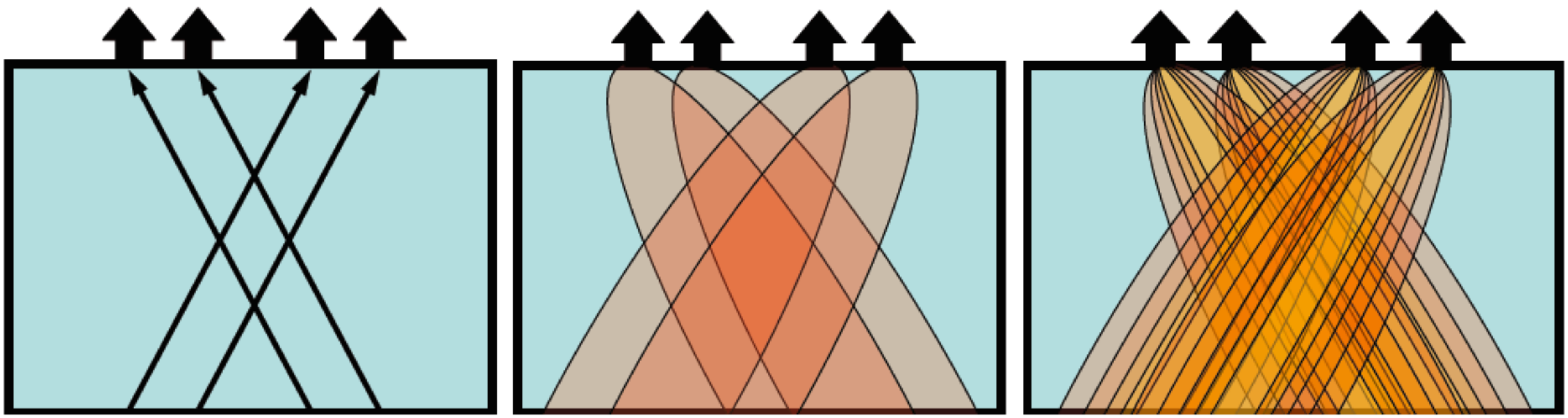

Ray theory: no constraints between the narrow rays (and there is a modeling error)

Finite-frequency, first generation: same number of constraints but no modeling error.

Finite-frequency, second generation (multi-frequency): more constraints from the same broadband waveforms.

# Measurement sensitivities for dT and dA/A

filter → align → correct amplitude

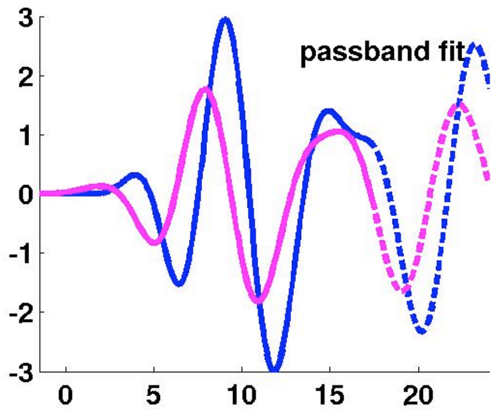


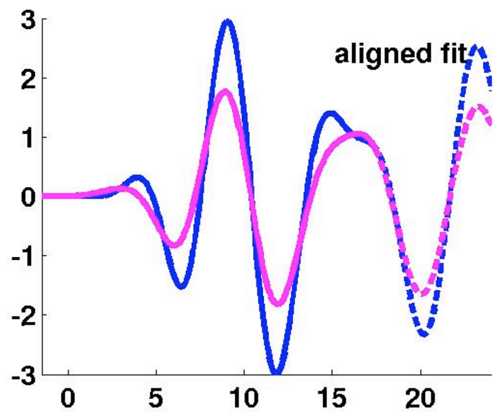


⇒ traveltime anomaly

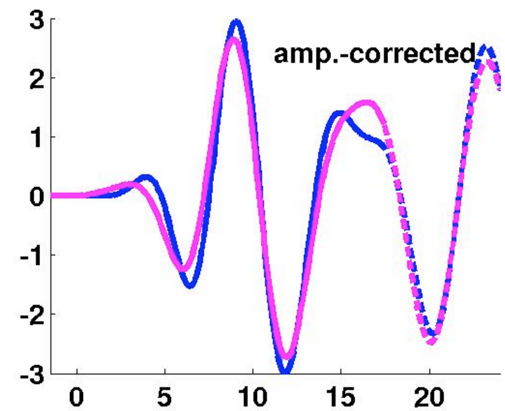


⇒ amplitude anomaly

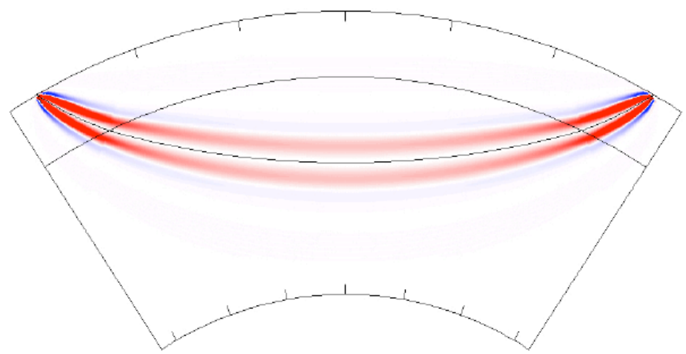

traveltime kernel, for a dominant period of 15 s

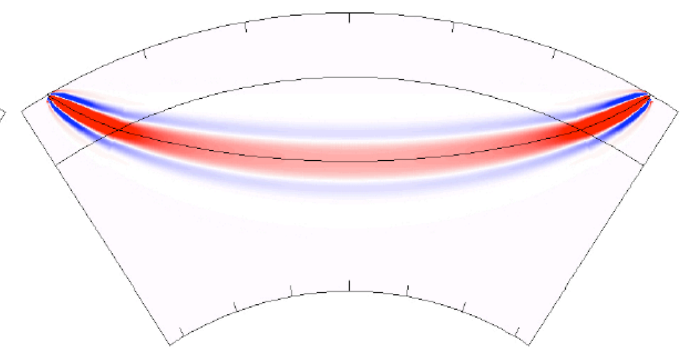

amplitude kernel (focusing)

# Modeling assumption for sensitivity computations: Single scattering (Born approximation)

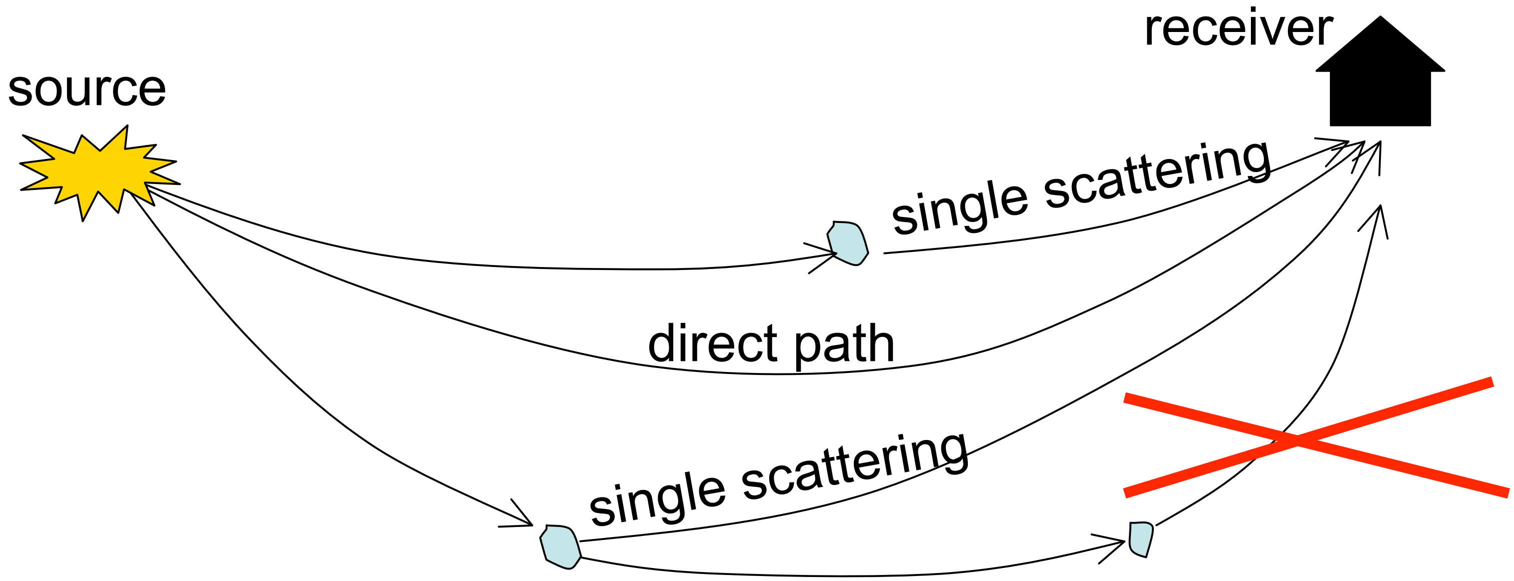


Energy contribution from multiple scattering assumed to be negligible.

Computation of sensitivity kernels:

1st generation implementation: paraxial ray tracing (Dahlen et al. 2000).

2nd generation: interaction of full numerical wavefields, forward and backward (Nissen-Meyer et al. 2007).

# How a P-wavetrain senses the mantle

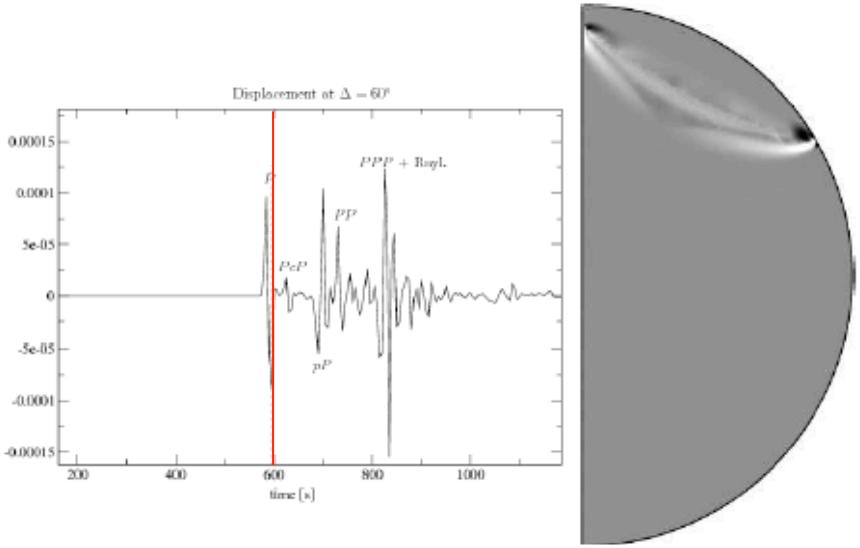


Nissen-Meyer et al. (2008)

# How a P-wavetrain senses the mantle

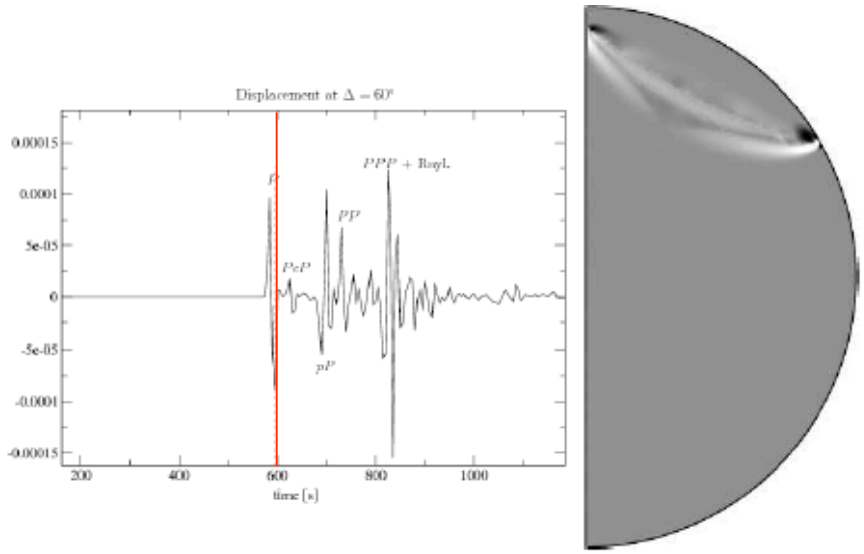


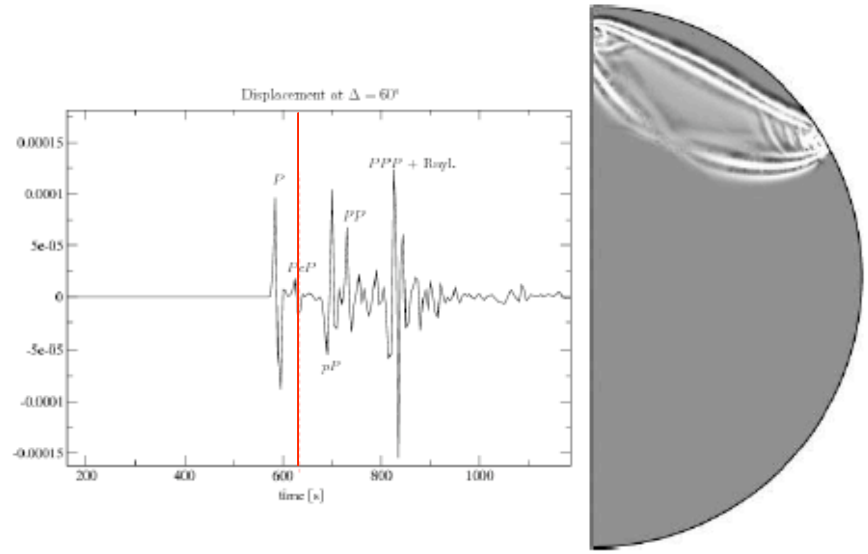


Nissen-Meyer et al. (2008)

# How a P-wavetrain senses the mantle

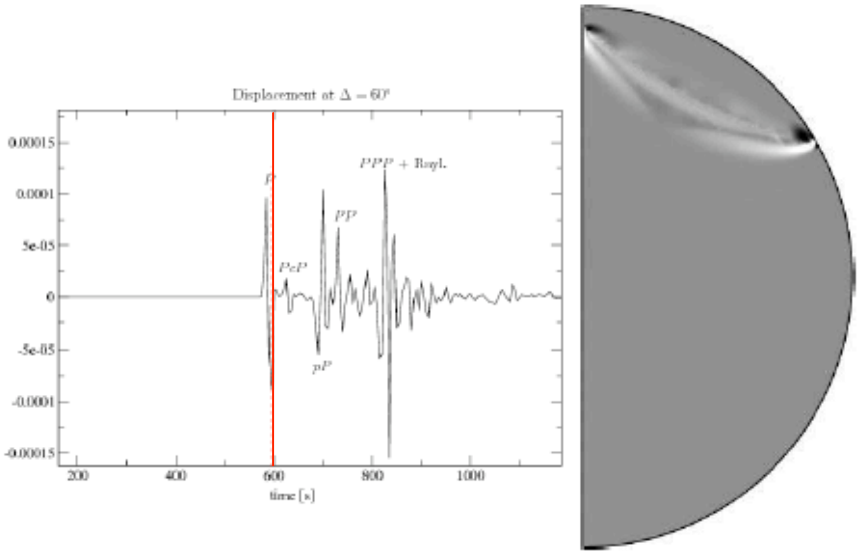


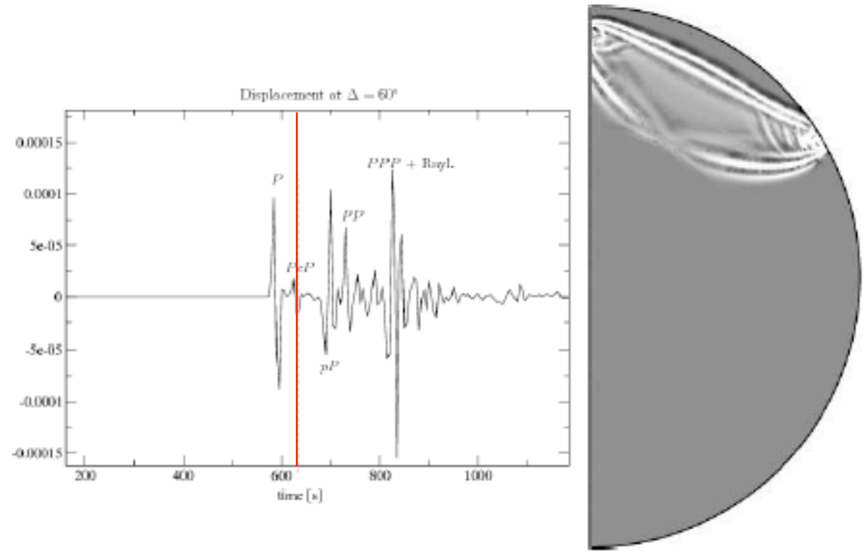


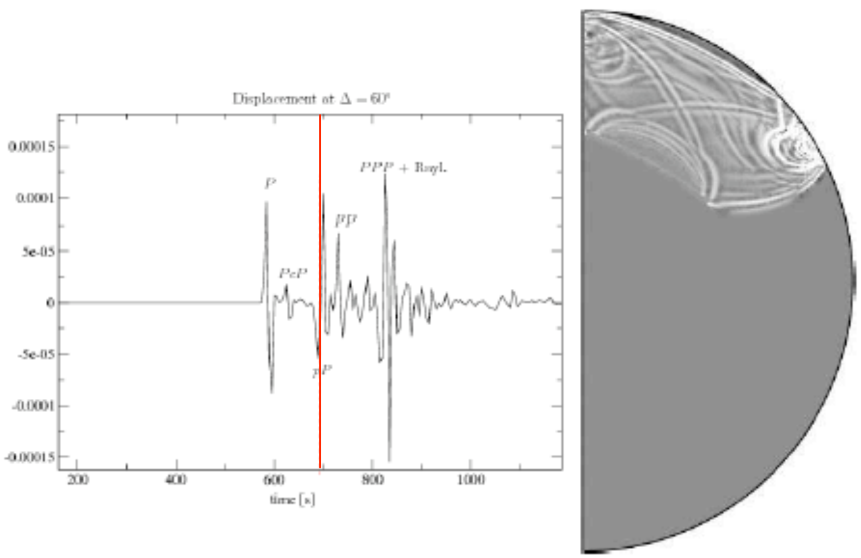


Nissen-Meyer et al. (2008)

# How a P-wavetrain senses the mantle

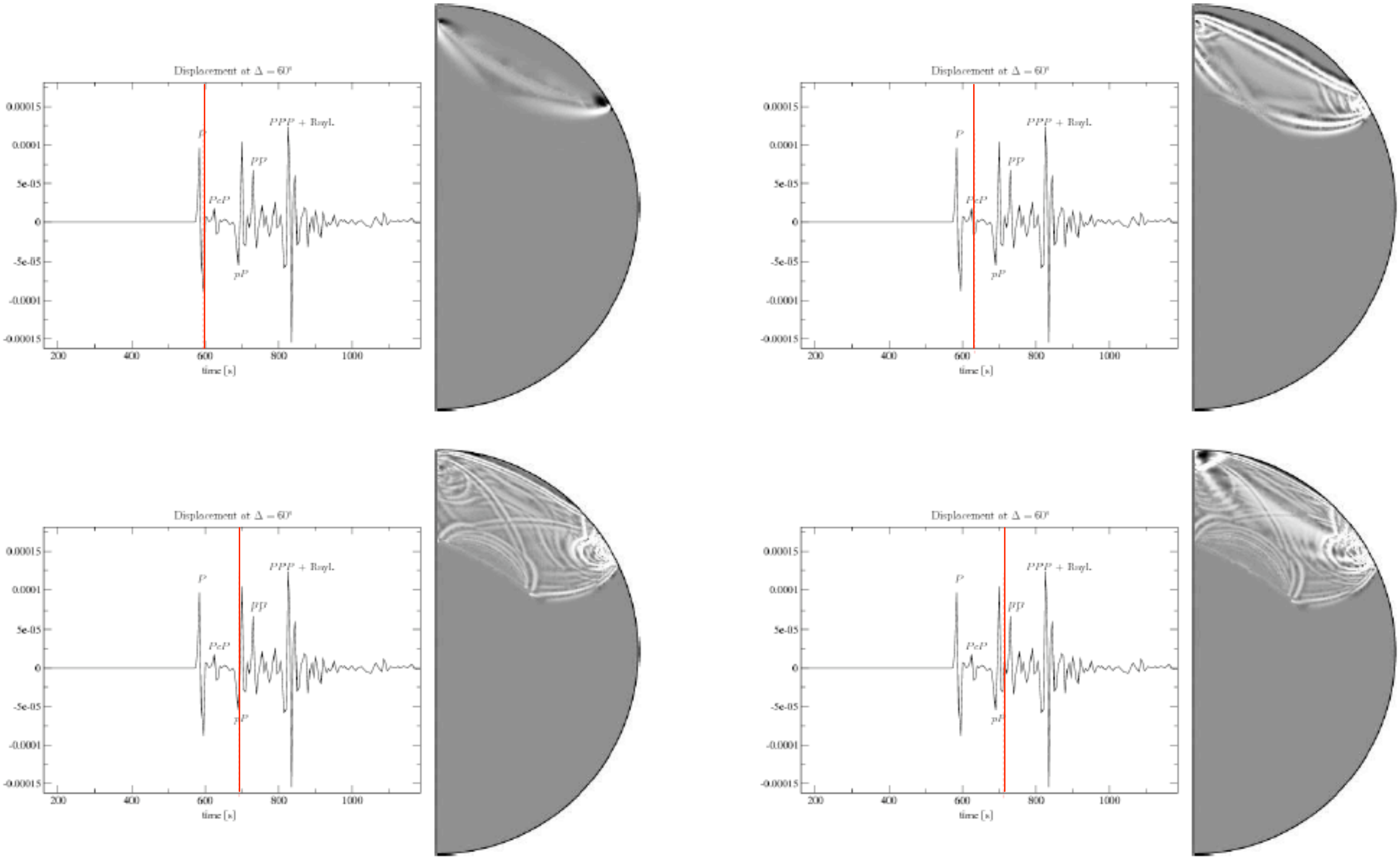


Nissen-Meyer et al. (2008)

# Sensitivities from full 3-D SEM wavefields

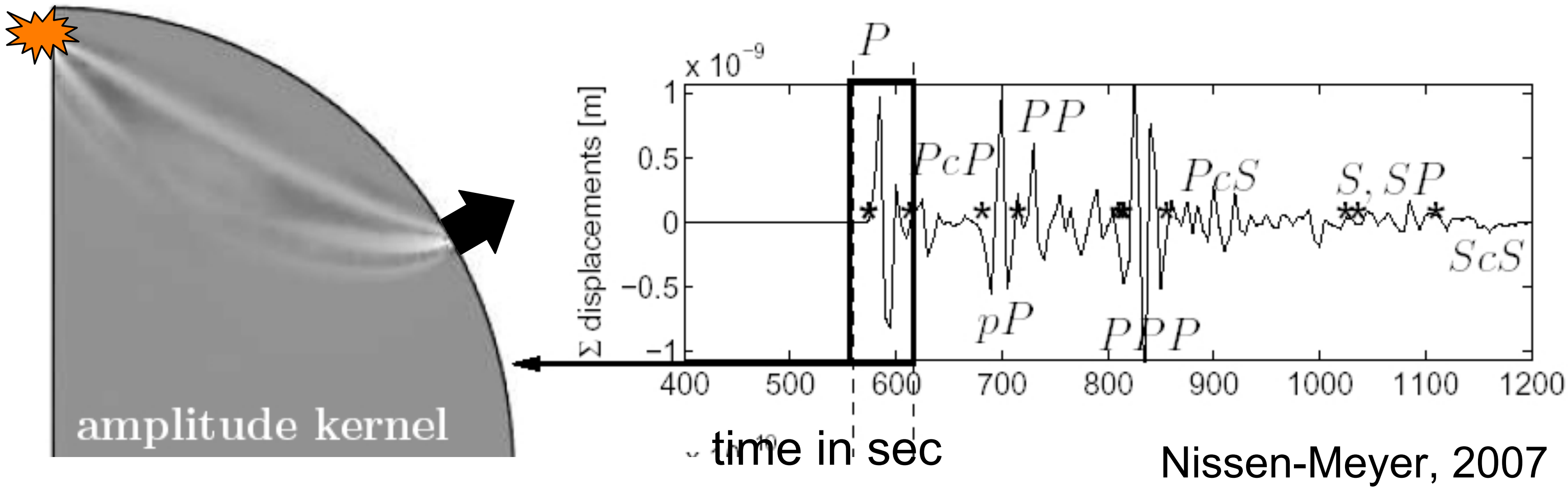


•Kernels from interaction of a forward with a backward wavefield at every hypothetical scattering location.

•Still a perturbational approach (like adjoint method).

•Extreme computational efficiency: exploiting spherically symmetric geometry of reference model → kernels to the highest naturally occuring frequencies (1-2 sec for teleseismic P-waves).

# Kernels and computational mesh

Global mesh of irregular tetrahedra

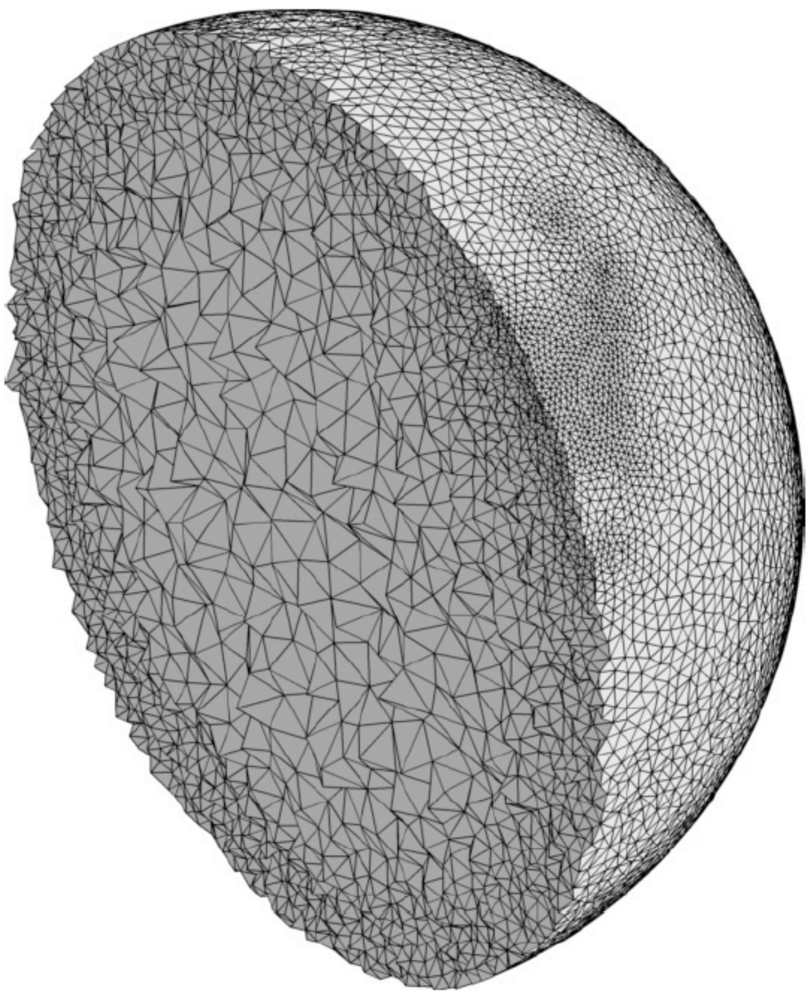

Top: traveltime kernel, bottom: amplitude kernel (focusing), both for a dominant period of 15 s

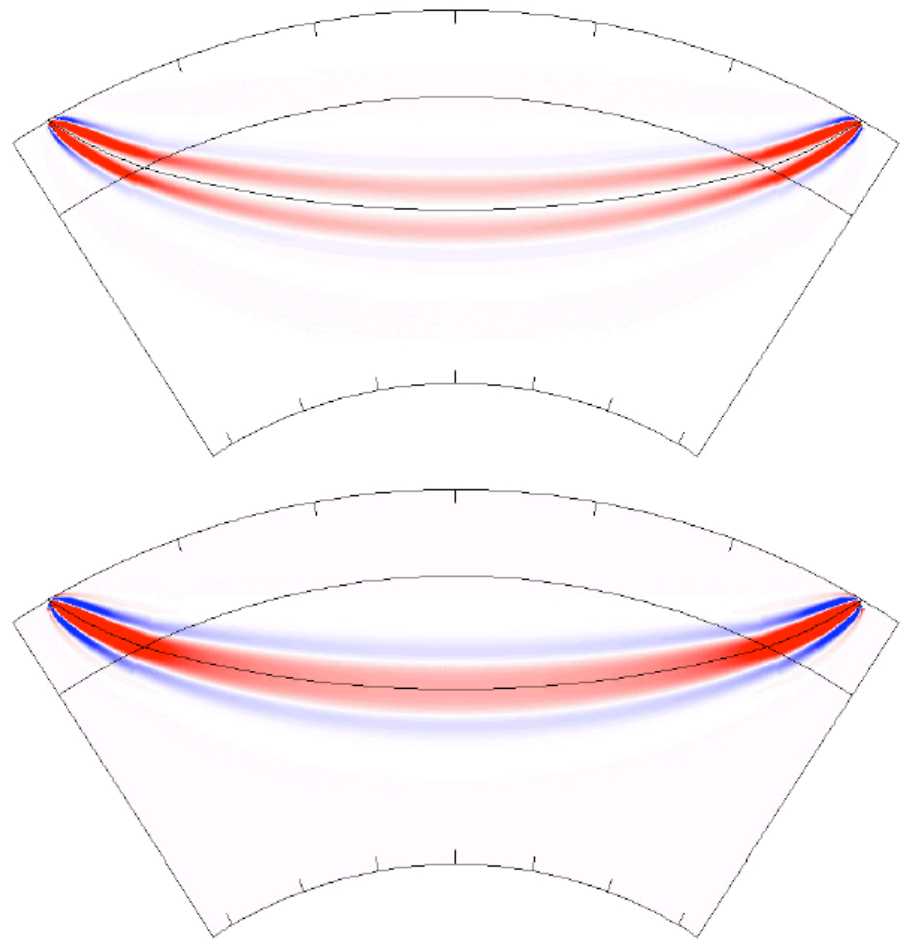

# Joint inversion of traveltime and amplitude anomalies

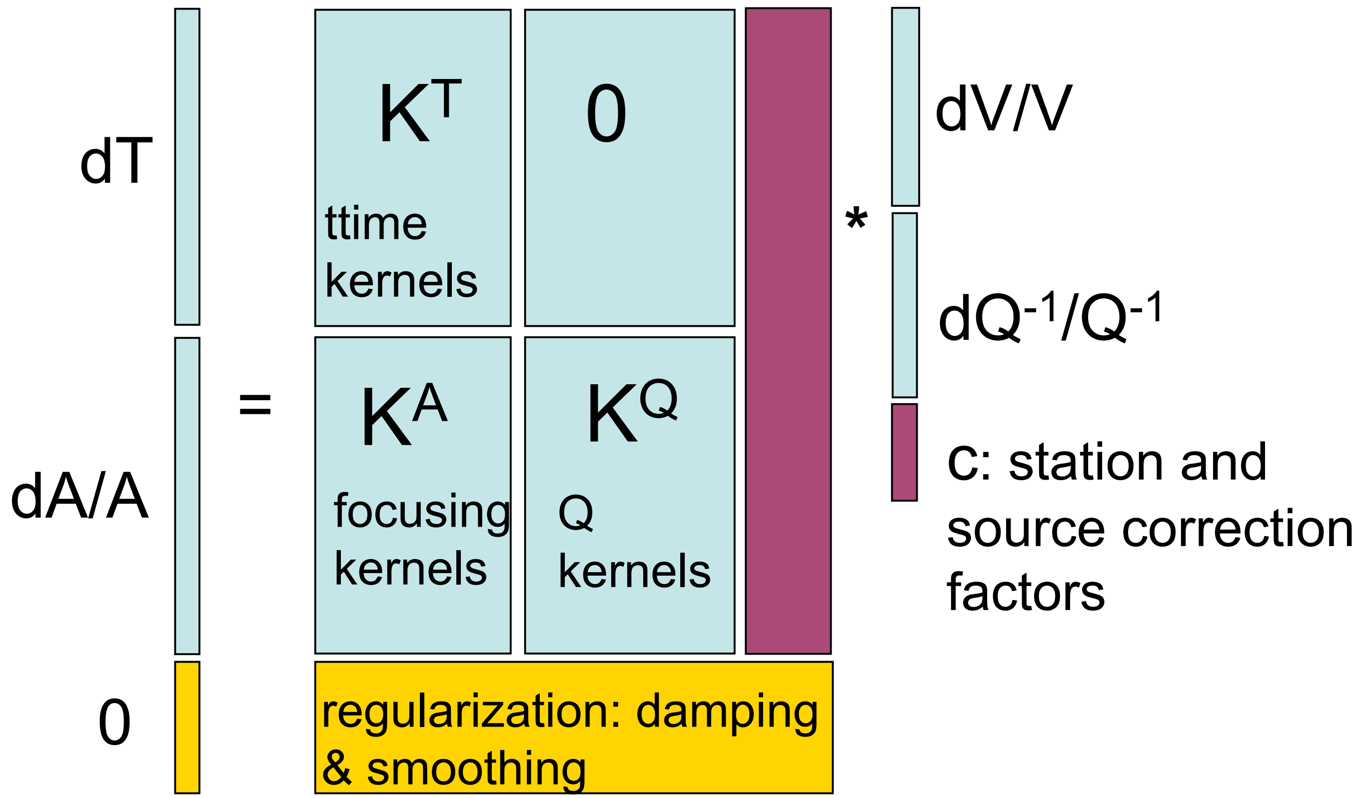


$dT_{obs} = dT_{dV}$ + source_correction + noise

$dA/A_{obs} = dA/A_{dV} + dA/A_{dQ}$ + source_cor + station_cor + noise

# Seismically fast material (subducted slabs) at 400-1800 km depth under North America

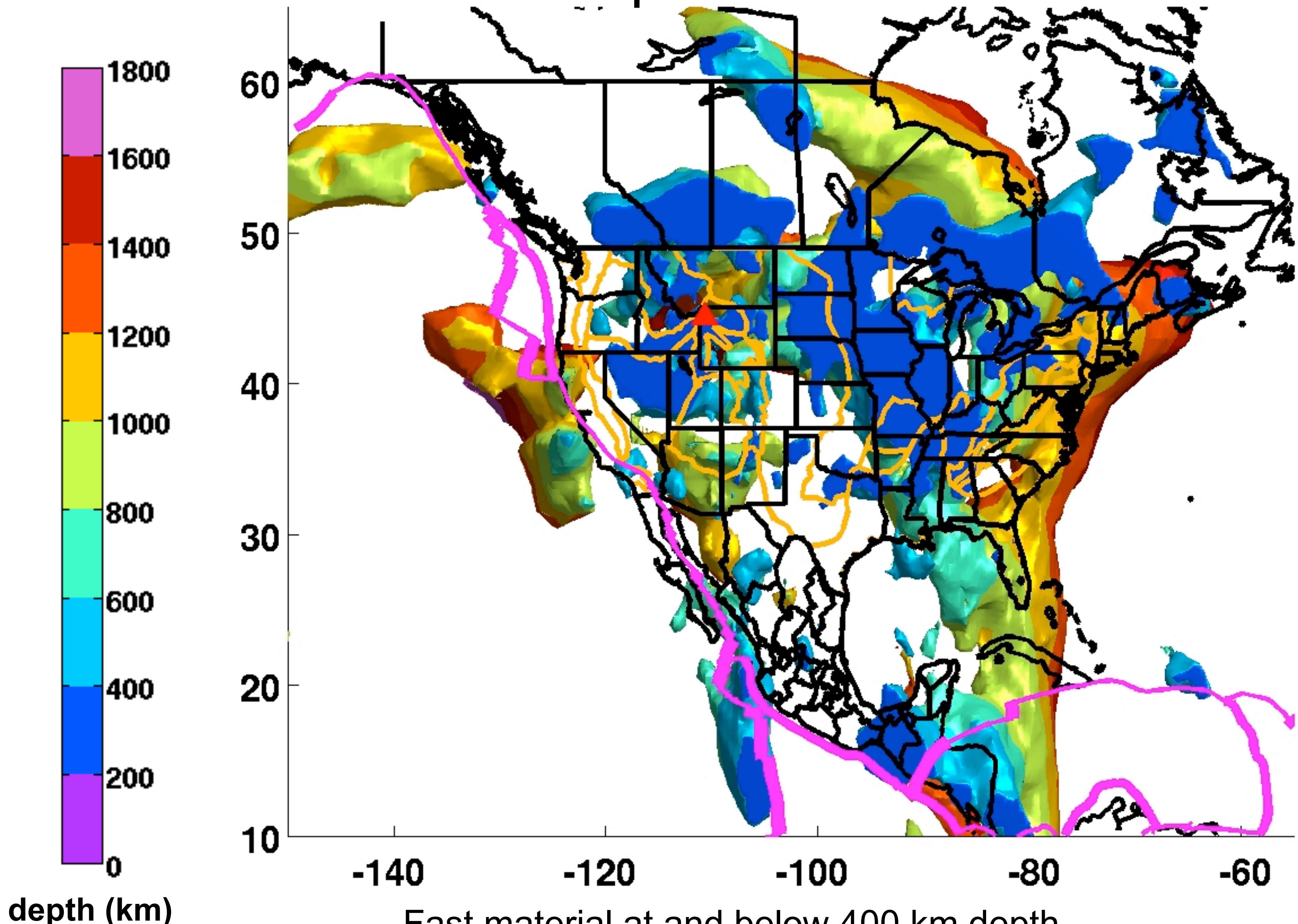


Fast material at and below 400 km depth

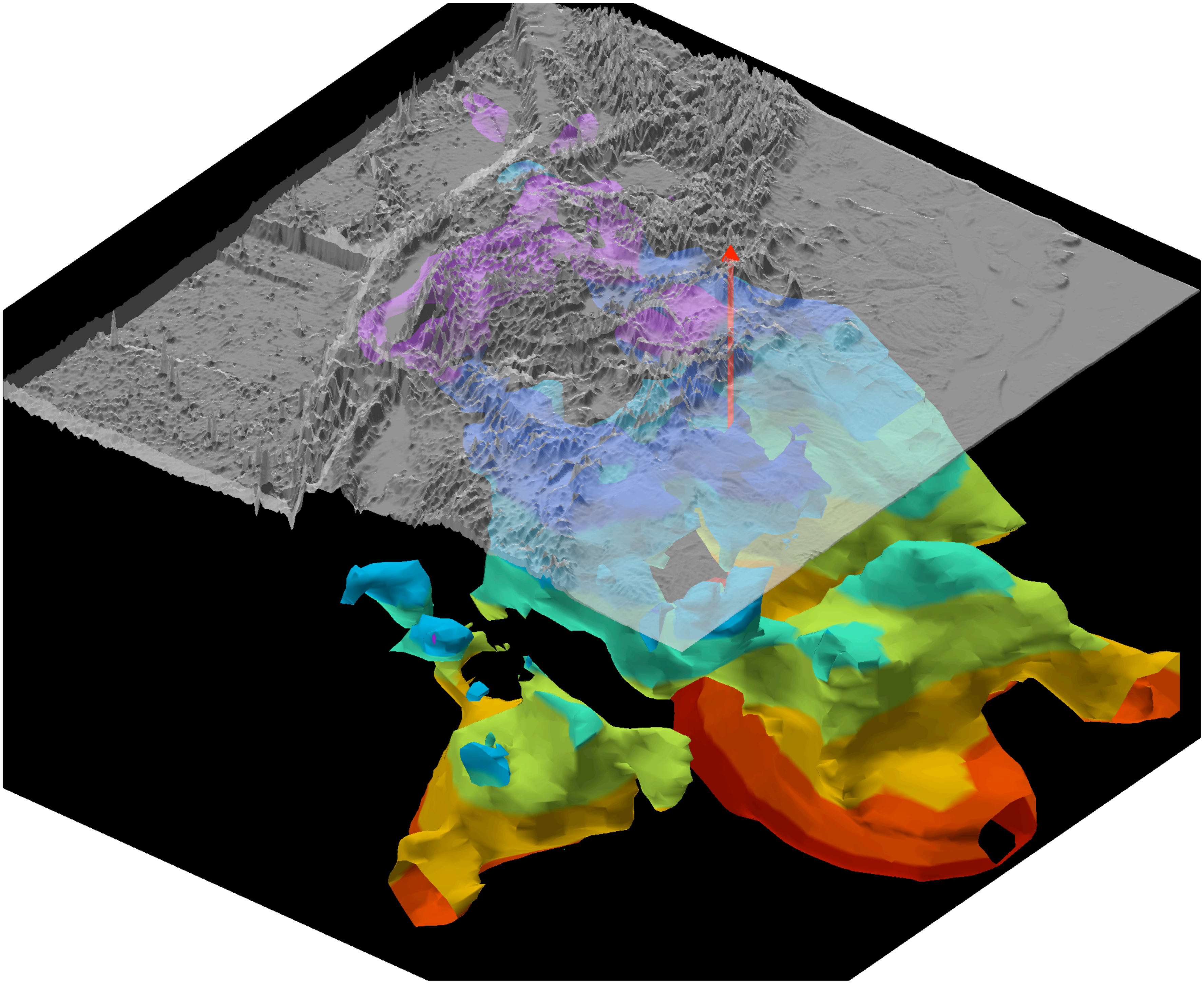

# Summary I

•Finite-frequency modeling spans the **entire exploitable frequency spectrum** of global-scale waves.

•Extreme computational efficiency through smart **exploitation of Earth's approximately spherical symmetry.**

•Original method for kernel computation was paraxial ray tracing. Is now becoming full SEM wave propagation.

•Point-to-point **kernels are explicitly computed and stored** ("kernel library" philosophy). Linear matrix inversion.

•Can deal with the full global database and its rapid growth. New data can be added at any time.

# Summary II

**Finite-frequency, first generation** was “better than traditional” P- and S-wave tomography (since wave scattering physics was included). Used existing data sets.

**Second generation** = new kinds of tomography: diffracted and triplicated waves, amplitude and topography kernels,… thanks to sensitivities from full numerical wavefield modeling.

Uses tailored, systematically frequency-dependent body-wave data (“multi-frequency tomography”).

# Waveform-based tomography methods are converging…old names remain confusing

"Full Waveform Inversion" and "Finite-Frequency Tomography" both:

•Model wave scattering in a perturbational approach.

•Do NOT invert full waveforms. Instead, robust misfit functionals derived from full waveforms are used (phase misfits).

•Account for and exploit the finite-frequency character of seismograms.

•Have acquired their names by distinction from ray theory(?), rather than distinction from each other.

•Adjoint vs. forward-backward vs. paraxial ray tracing are pragmatic implementation choices, not fundamental differences.

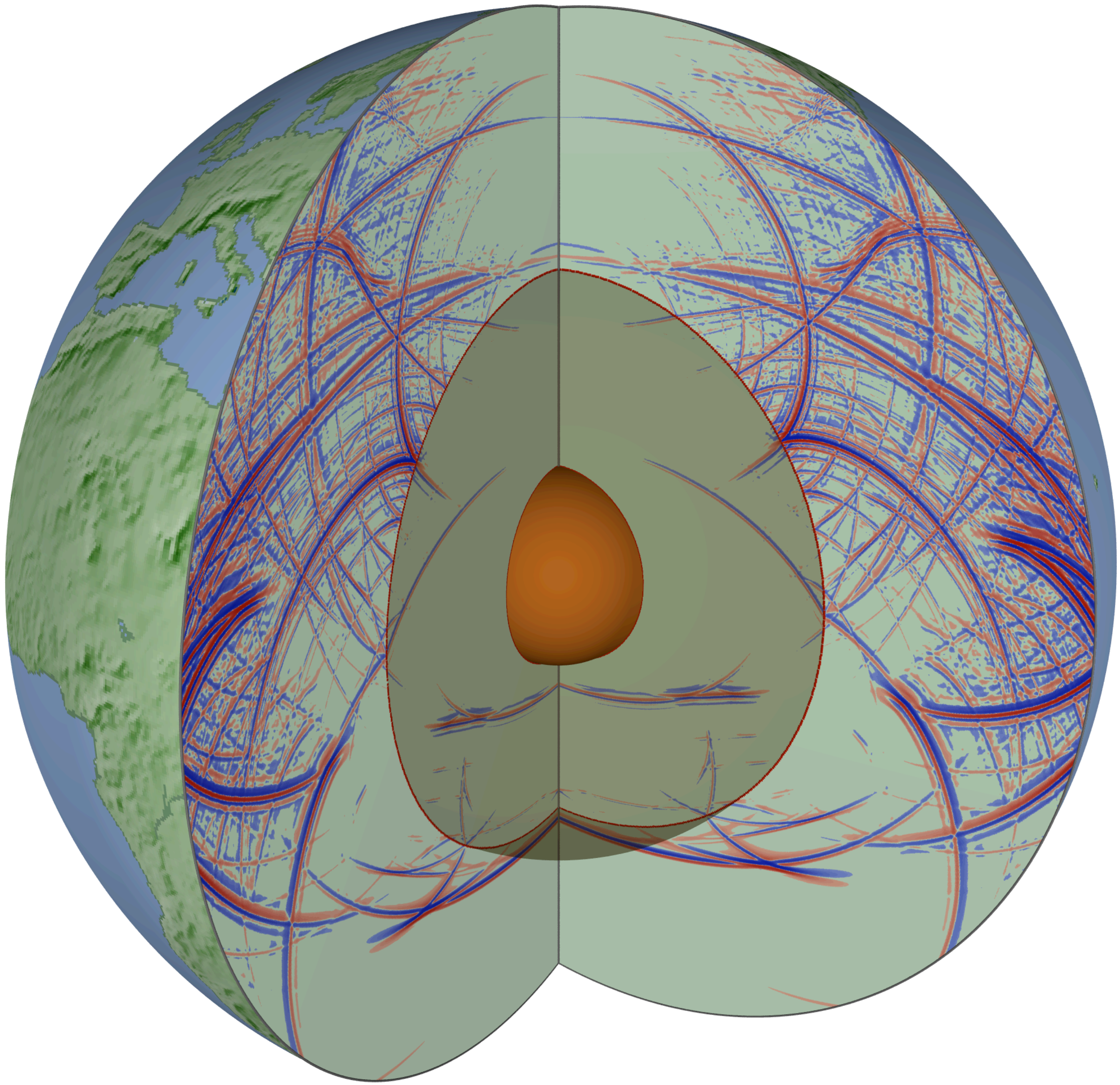

# Dispersive P-wave traveltimes for an earthquake from the Kurils

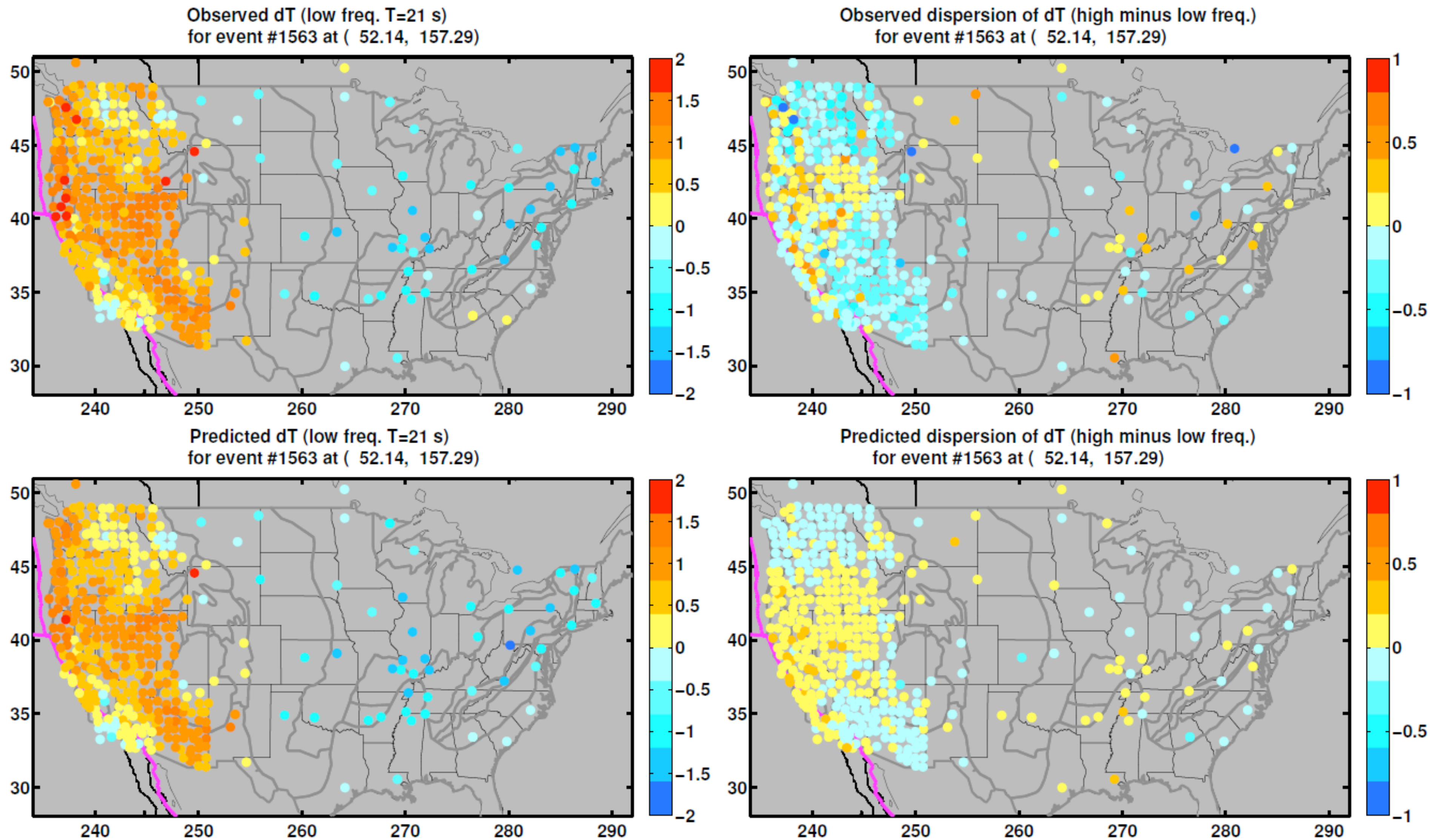

# Dispersive P-wave amplitudes for an earthquake from the Kurils

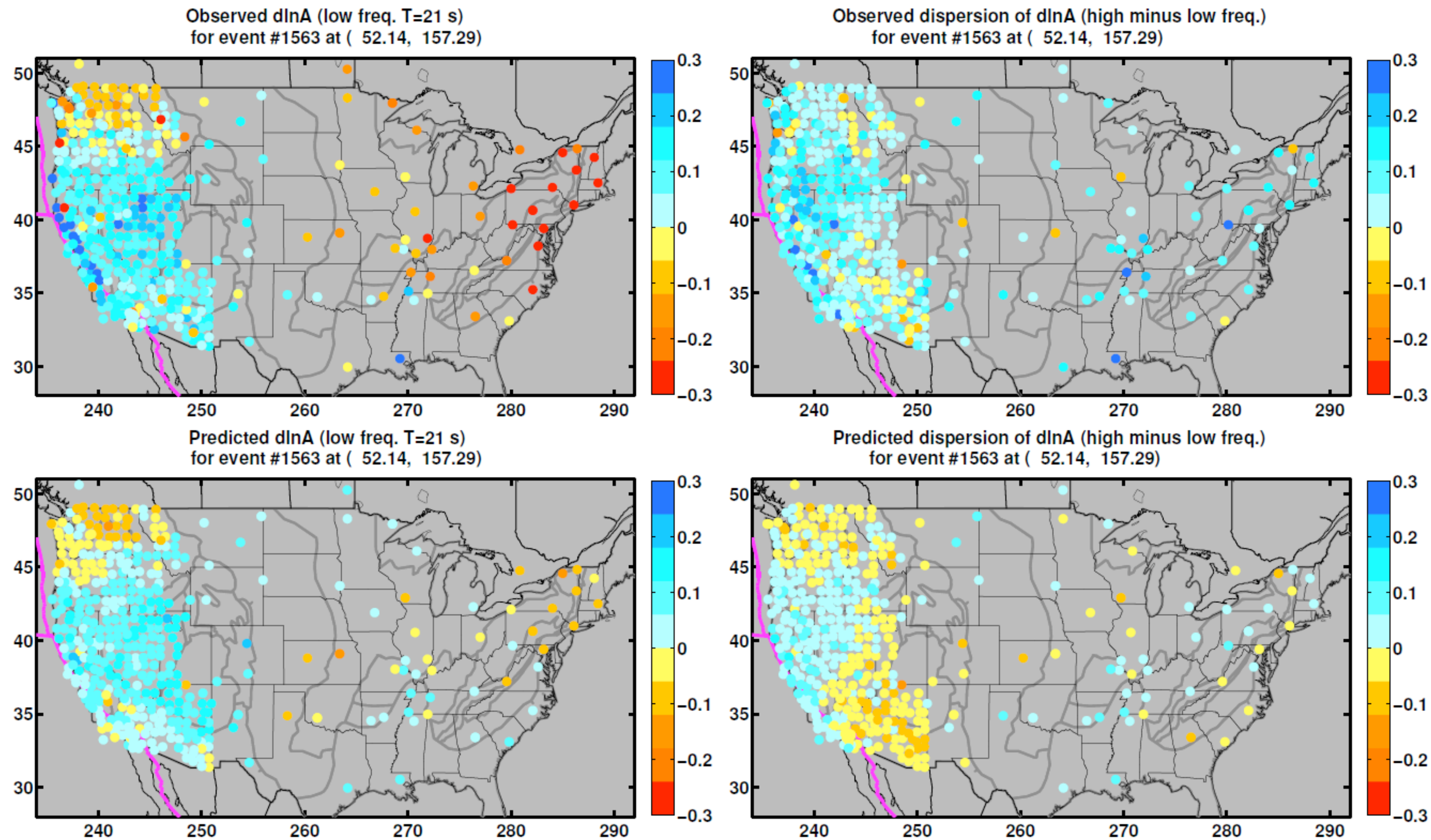

# Traveltime dispersion at an individual station

Station #576 (ISCO.) measured 215 events

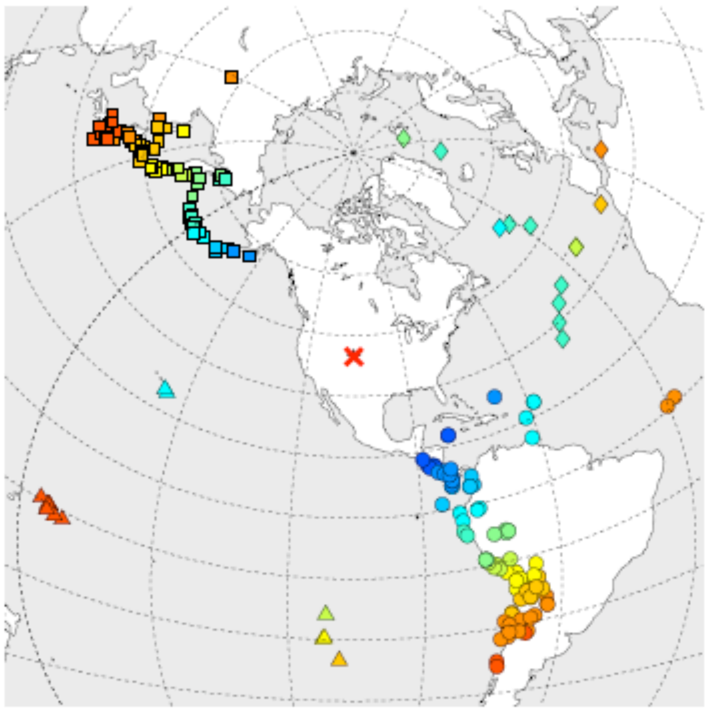

ISCO: Idaho Springs in Colorado

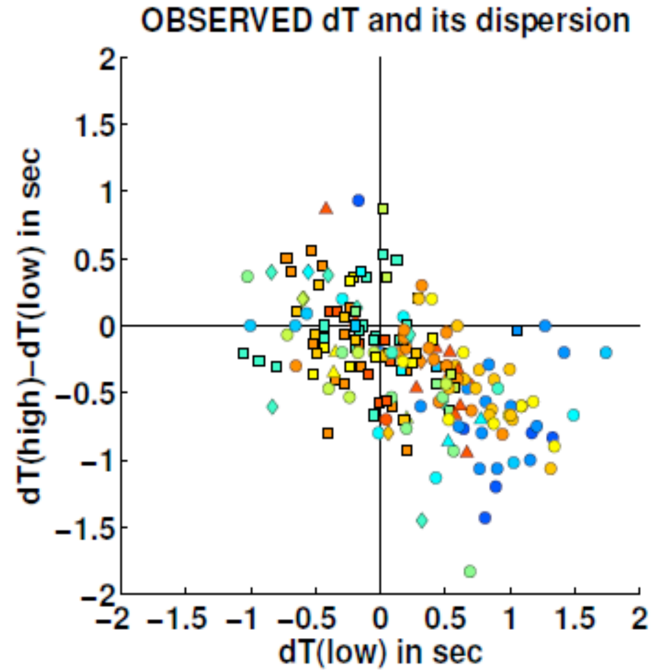


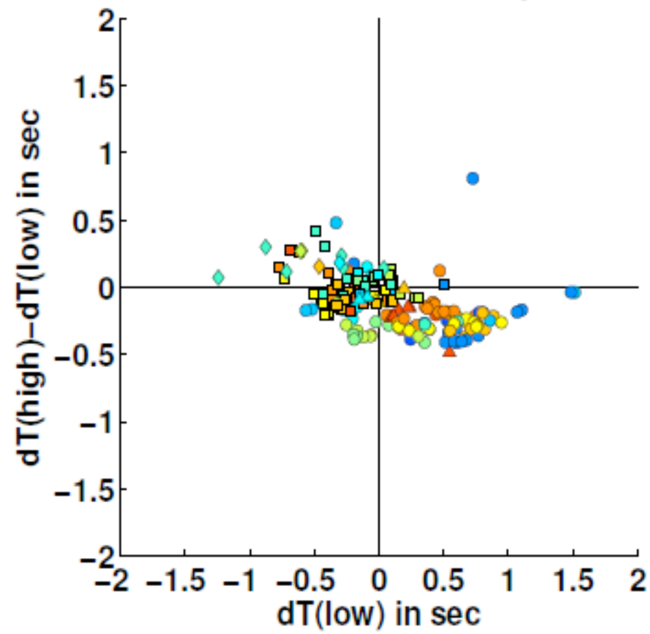


x-axis: dT($T_d$=21 s) lowest frequency band

y-axis: dT(4 s) – dT(21 s) highest minus lowest

# Source time functions

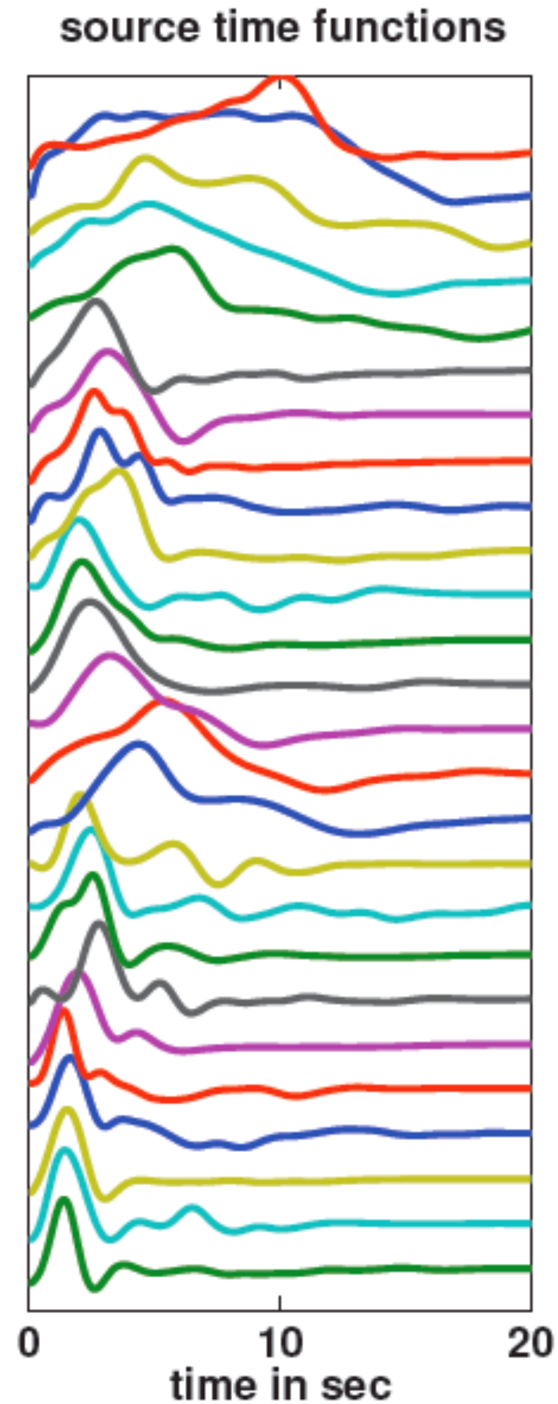

# P-velocity can be recovered from amplitudes only.

Depth = 60 km

Vp from traveltimes only

Vp from amplitudes only

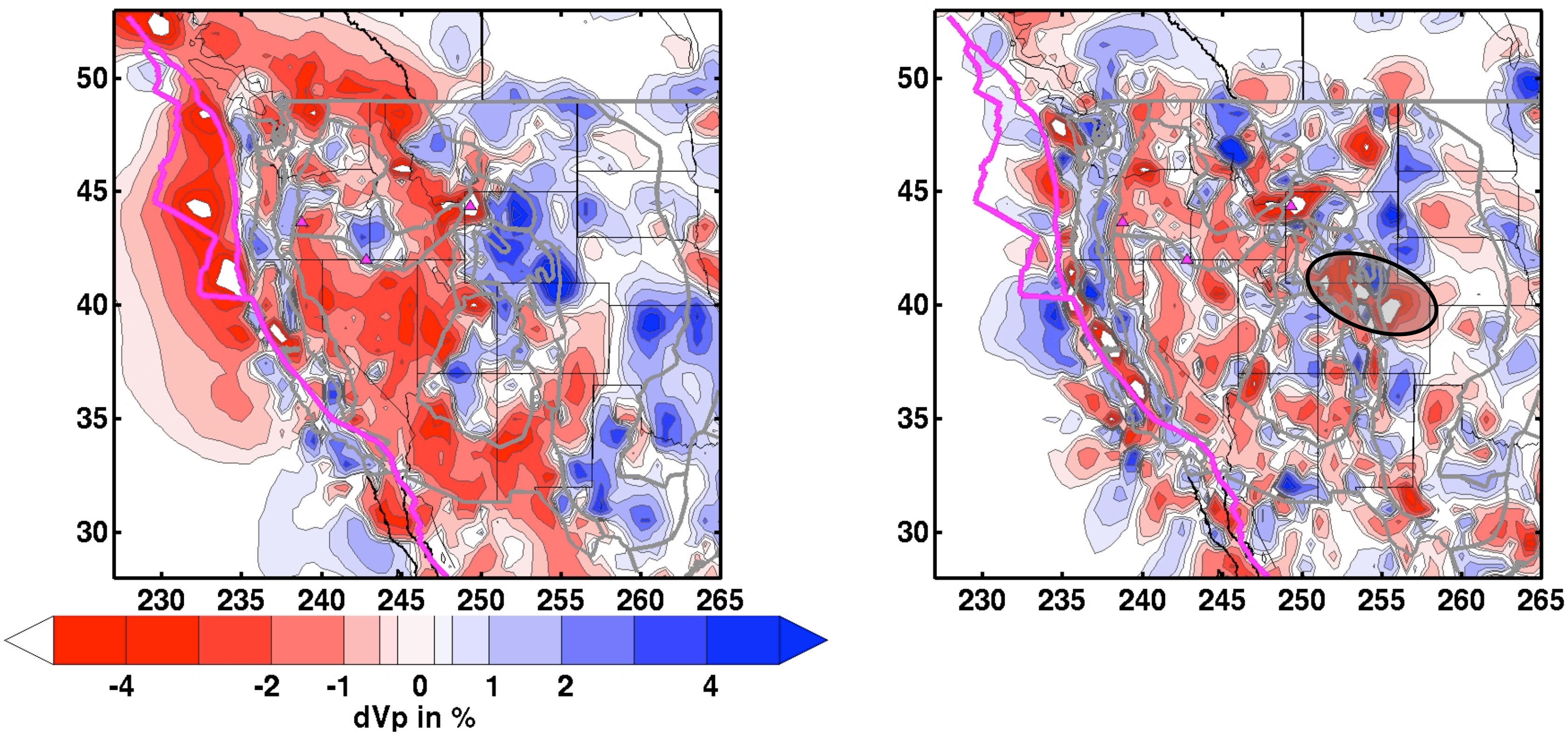

# P-velocity can be recovered from amplitudes only.

Depth = 700 km

Vp from traveltimes only

Vp from amplitudes only

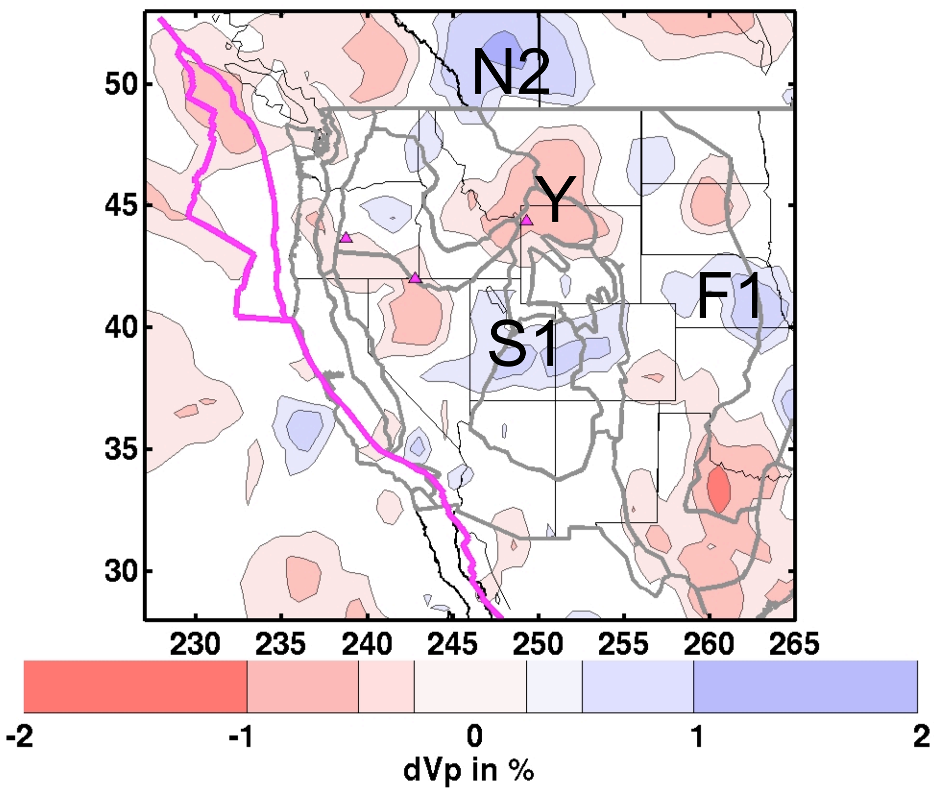


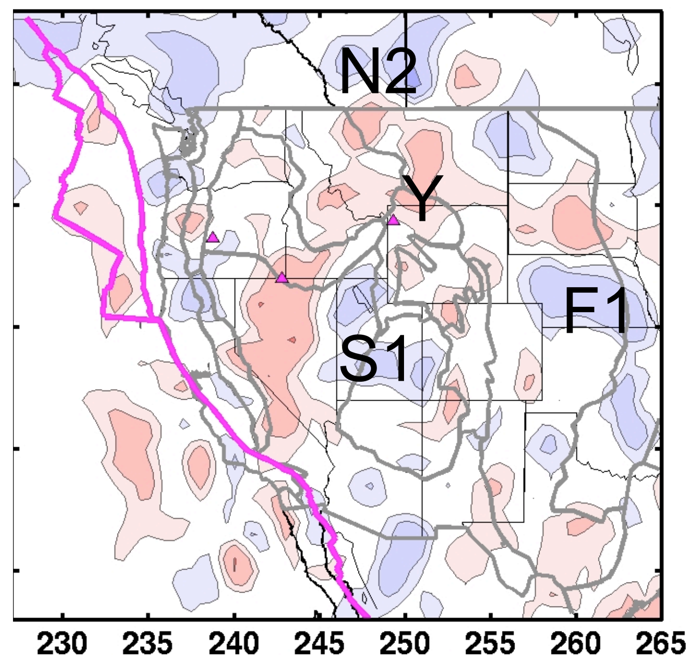

# P-velocity can be recovered from amplitudes only.

Section B: Snake River Plain

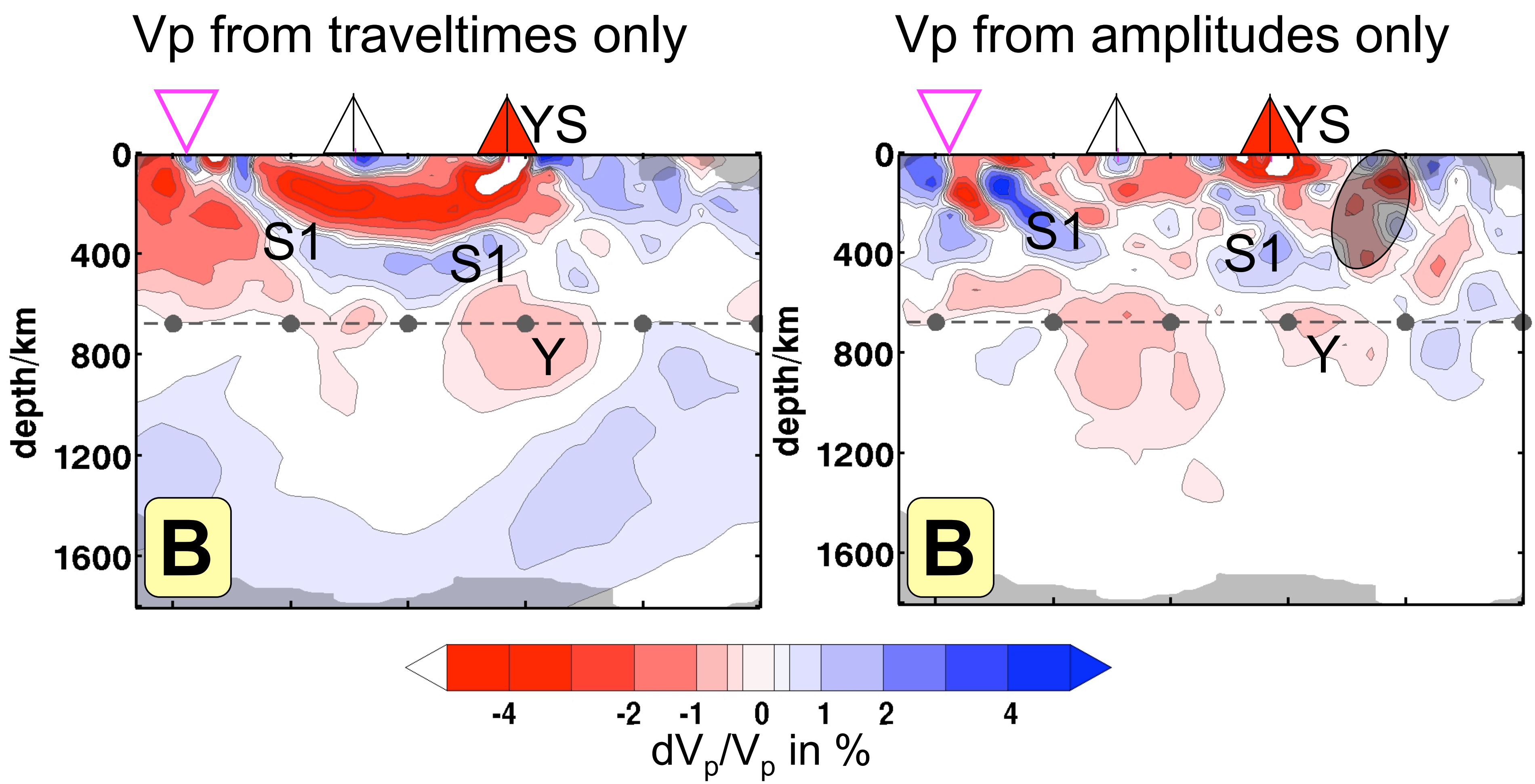

# Resolution ambiguity: moderate leakage of Vp into Qs (at 100 km depth)

recovered dVp/Vp in %

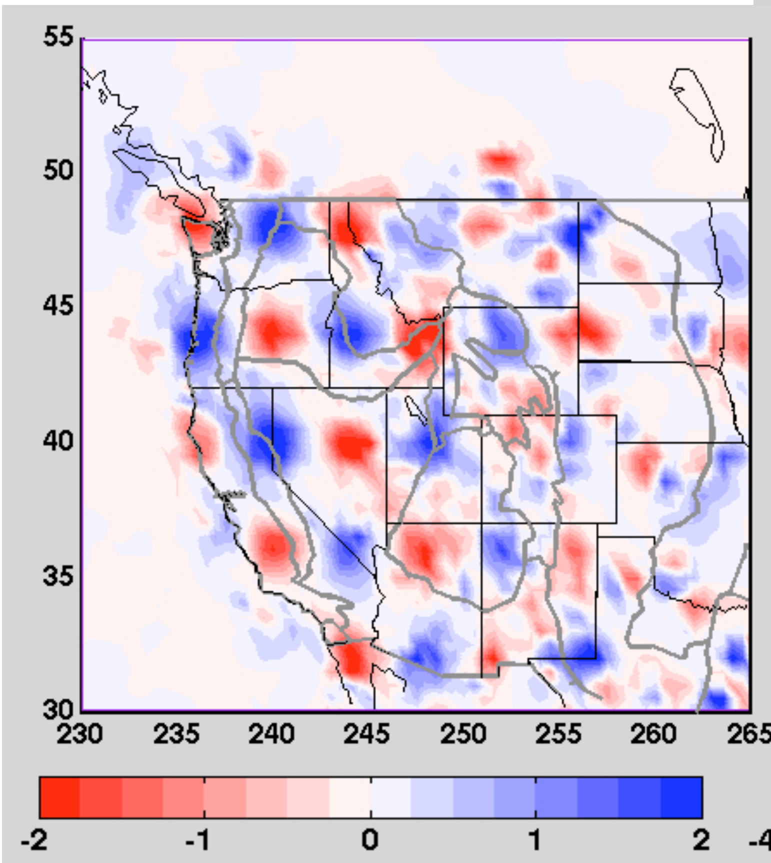


recovered dQs/Qs in %
(should be zero)

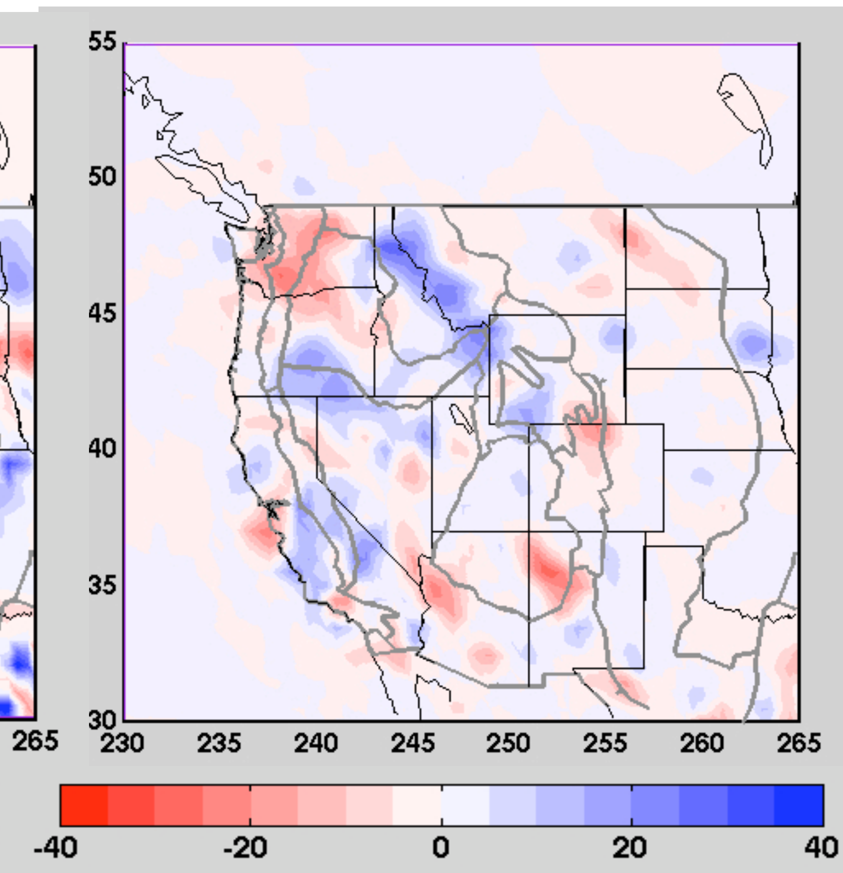

# Amplitude data

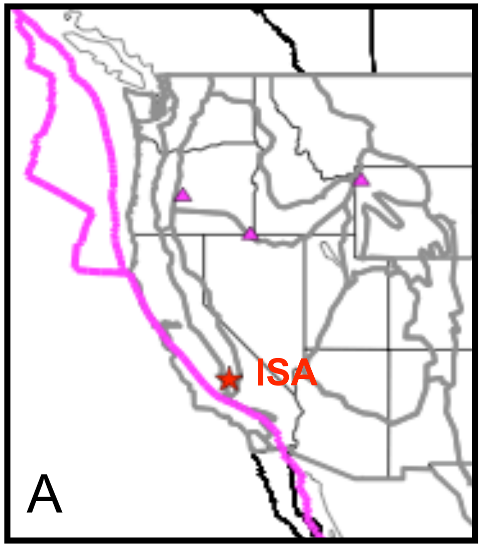


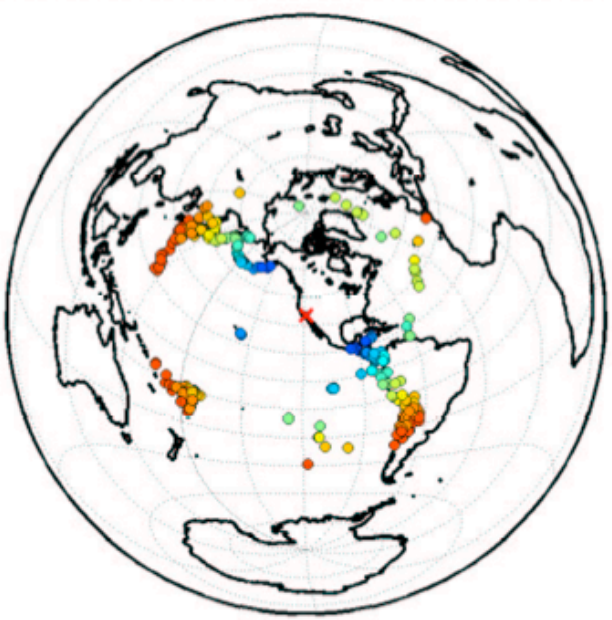

Example: Station ISA measured 299 events.

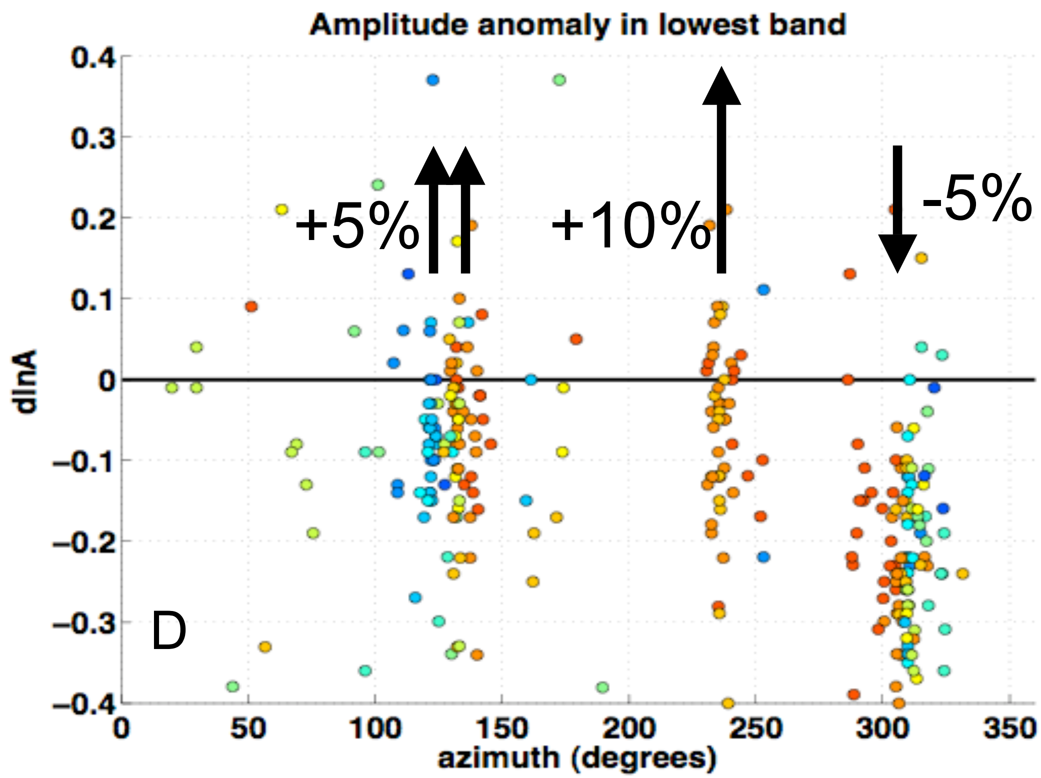


Amplitude anomalies dA/A in lowest band (21 s period). Arrows show trend (highest minus lowest band)

# Observed and predicted anomalies at station ISA

Observed dA/A

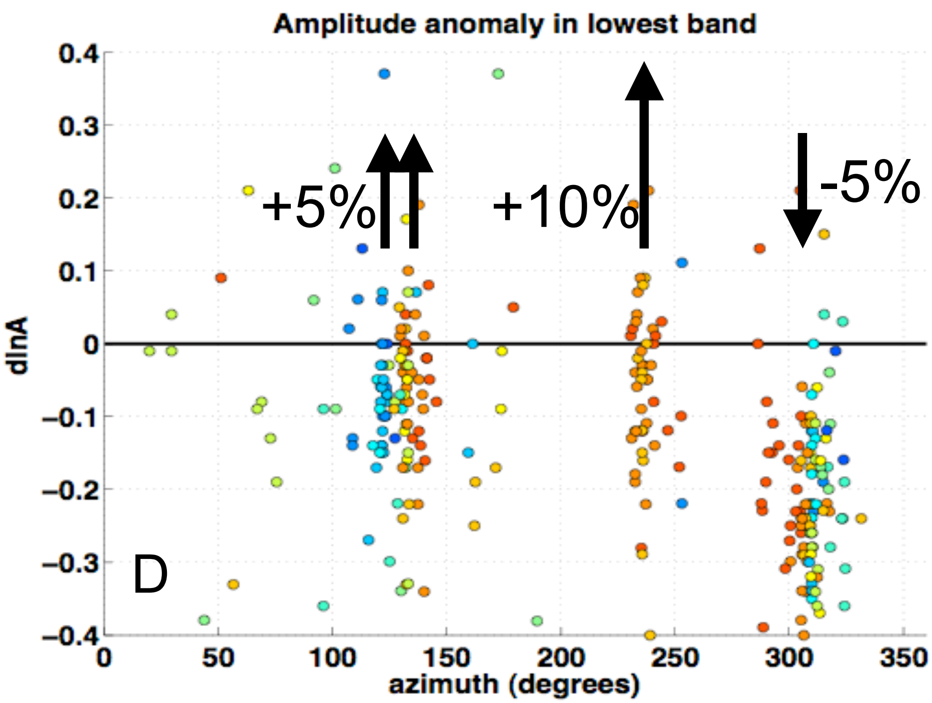


Predicted by Vp

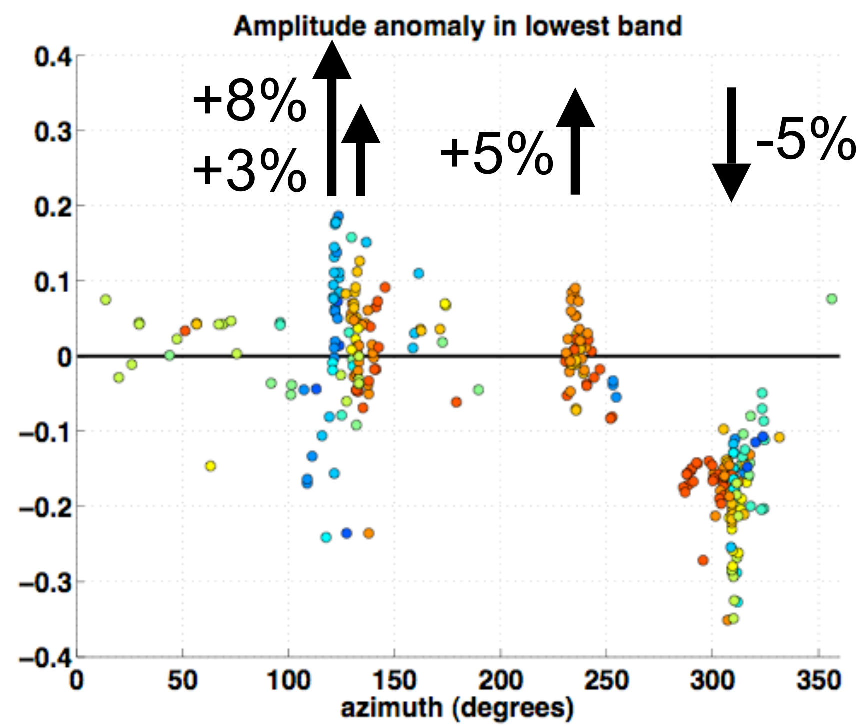


Amplitude anomalies dA/A in lowest band (20 s period). Arrows show trend (highest minus lowest band)

# Seismic tomography in one slide

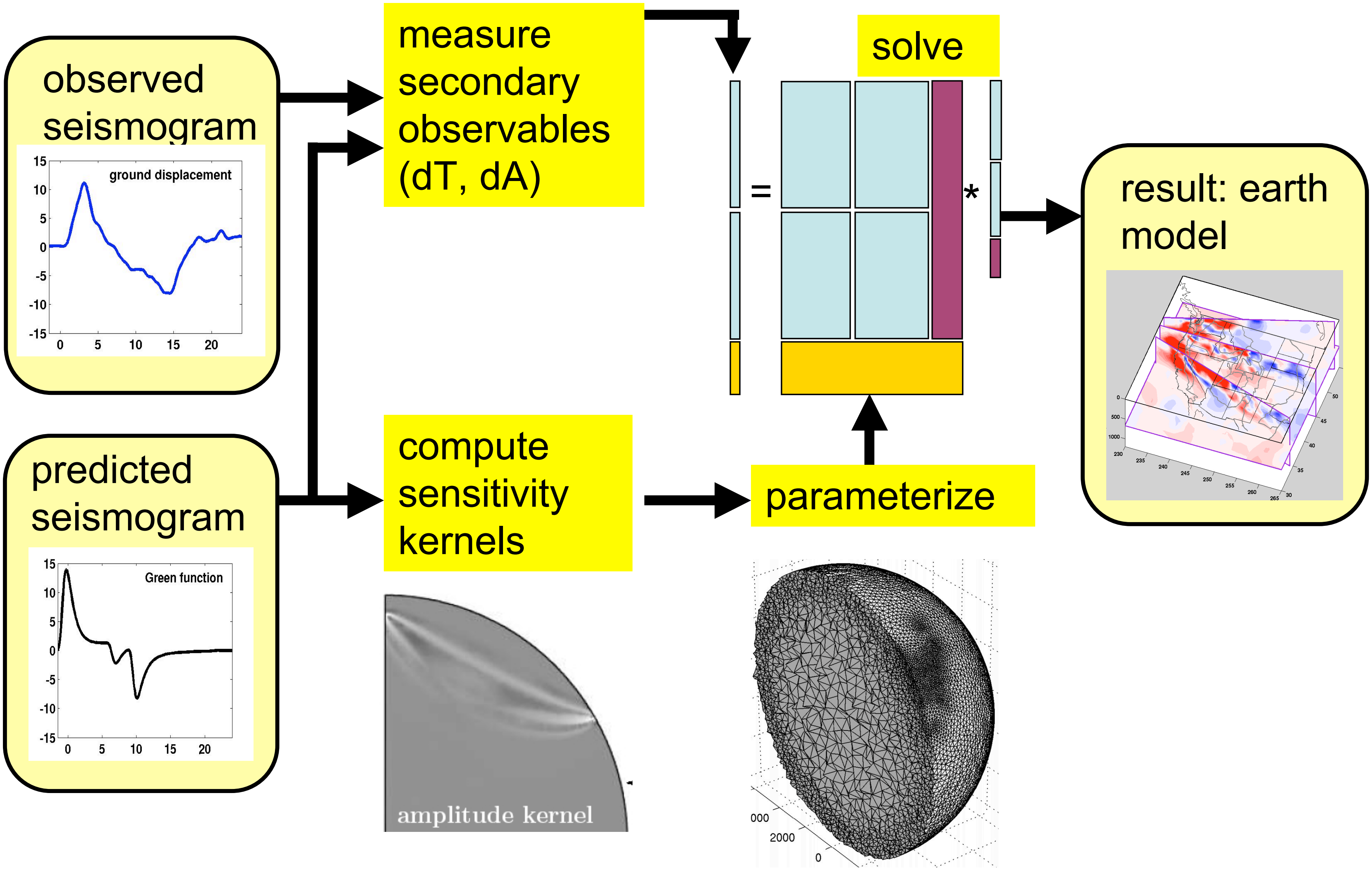

# Tomography result: a mantle model (for example under North America)

Result: three-dimensional model of mantle structure.

Maps of deviations of seismic velocities from the layered default model.

Blue: faster than expected. Red: slower (by a few percent)

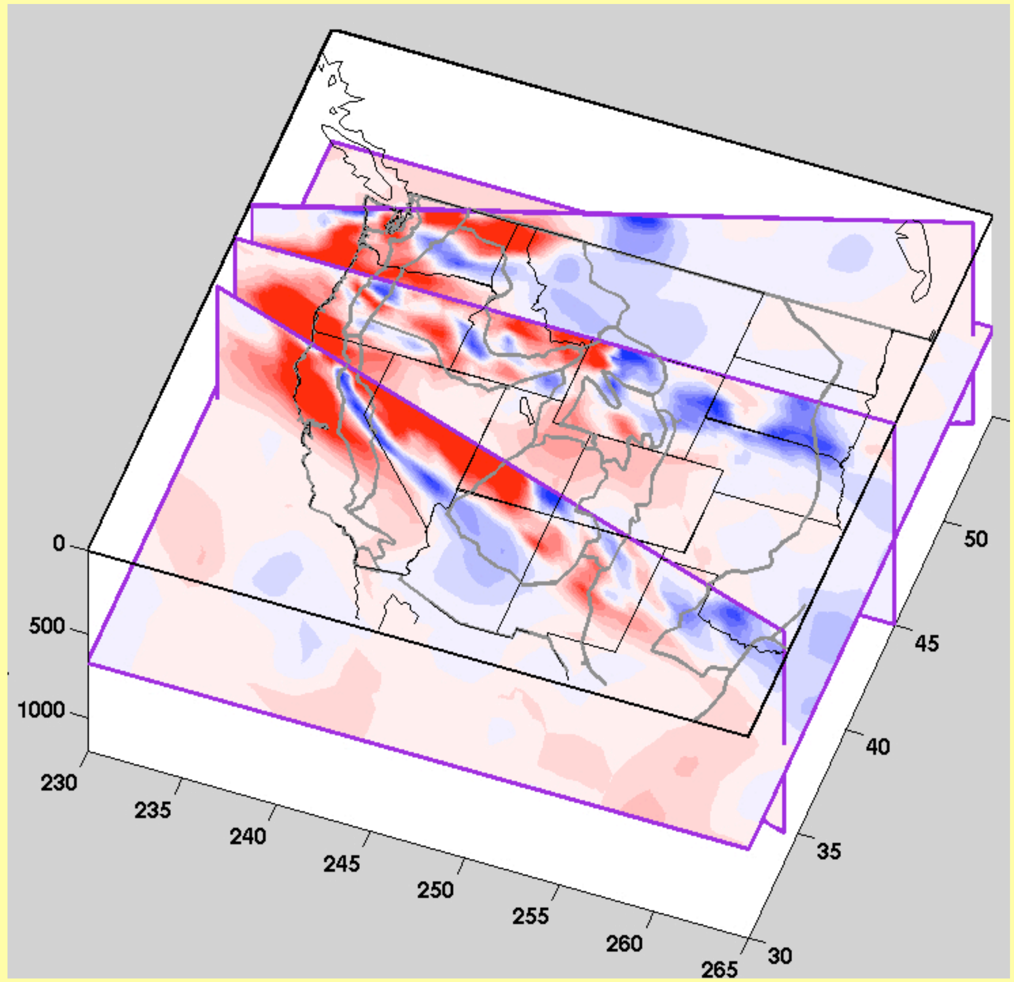

# Seismically fast material (= a subducted tectonic plate) beneath western North America

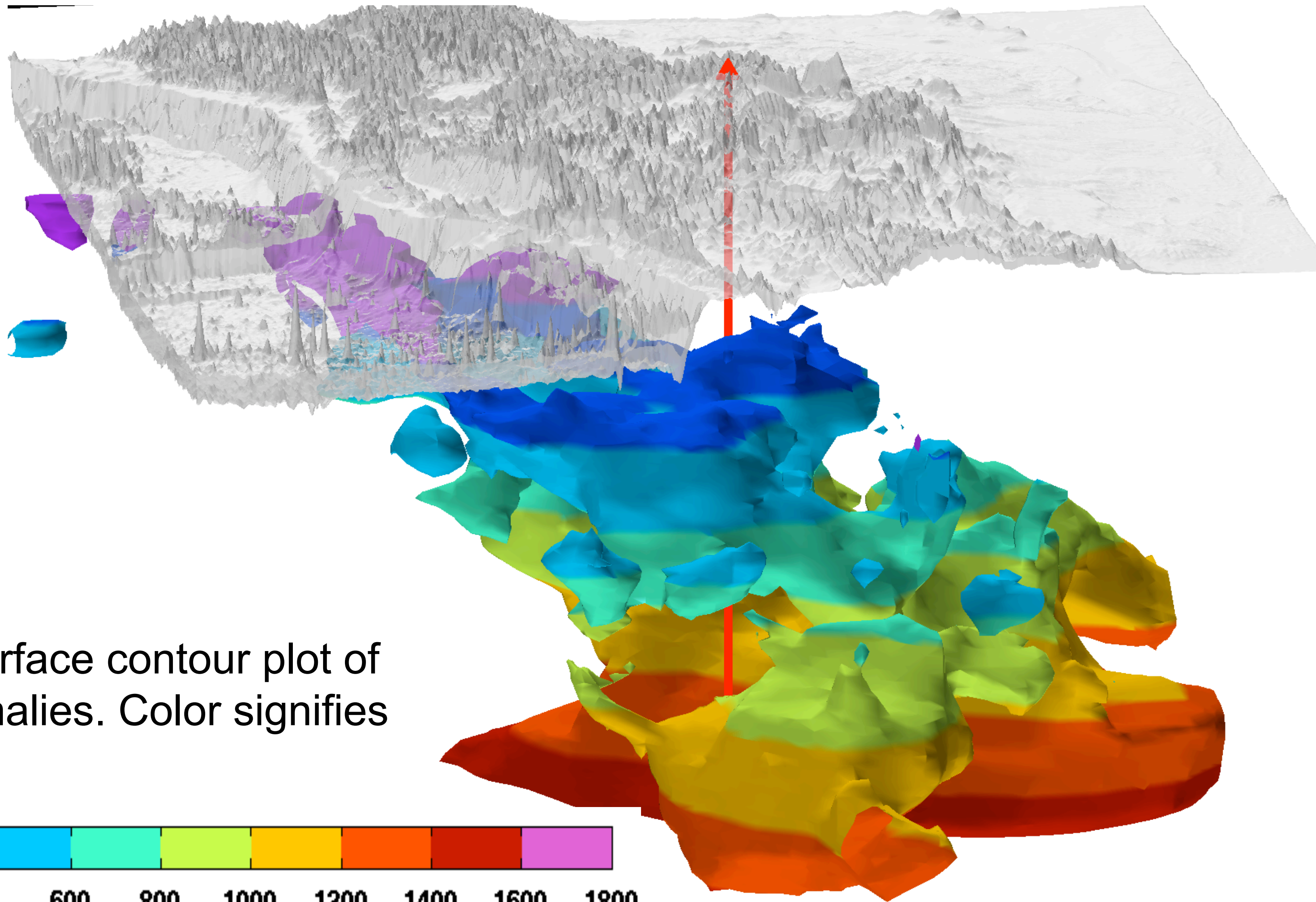

3-D isosurface contour plot of fast anomalies. Color signifies depth.

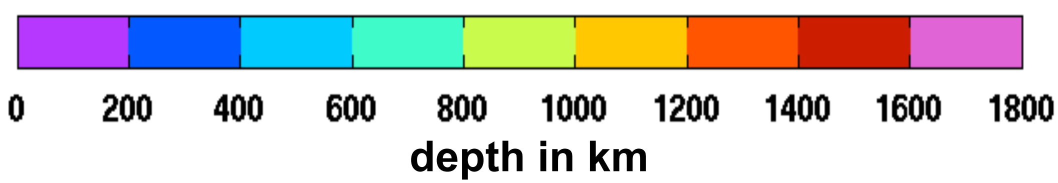

Camp FWI

Asterix, Tarantola, Pratt, Virieux, Igel, Fichtner, Tromp

Camp FF tomo

Obelix, Dahlen, Hung, Nolet, Montelli, Sigloch, Nissen-Meyer, Tian, Tromp

Fades out into bigger picture: Roemercamp ray theory, QUEST, scatter-brained seismologists, waveform-based

# All fast material (0-1800 km depth)

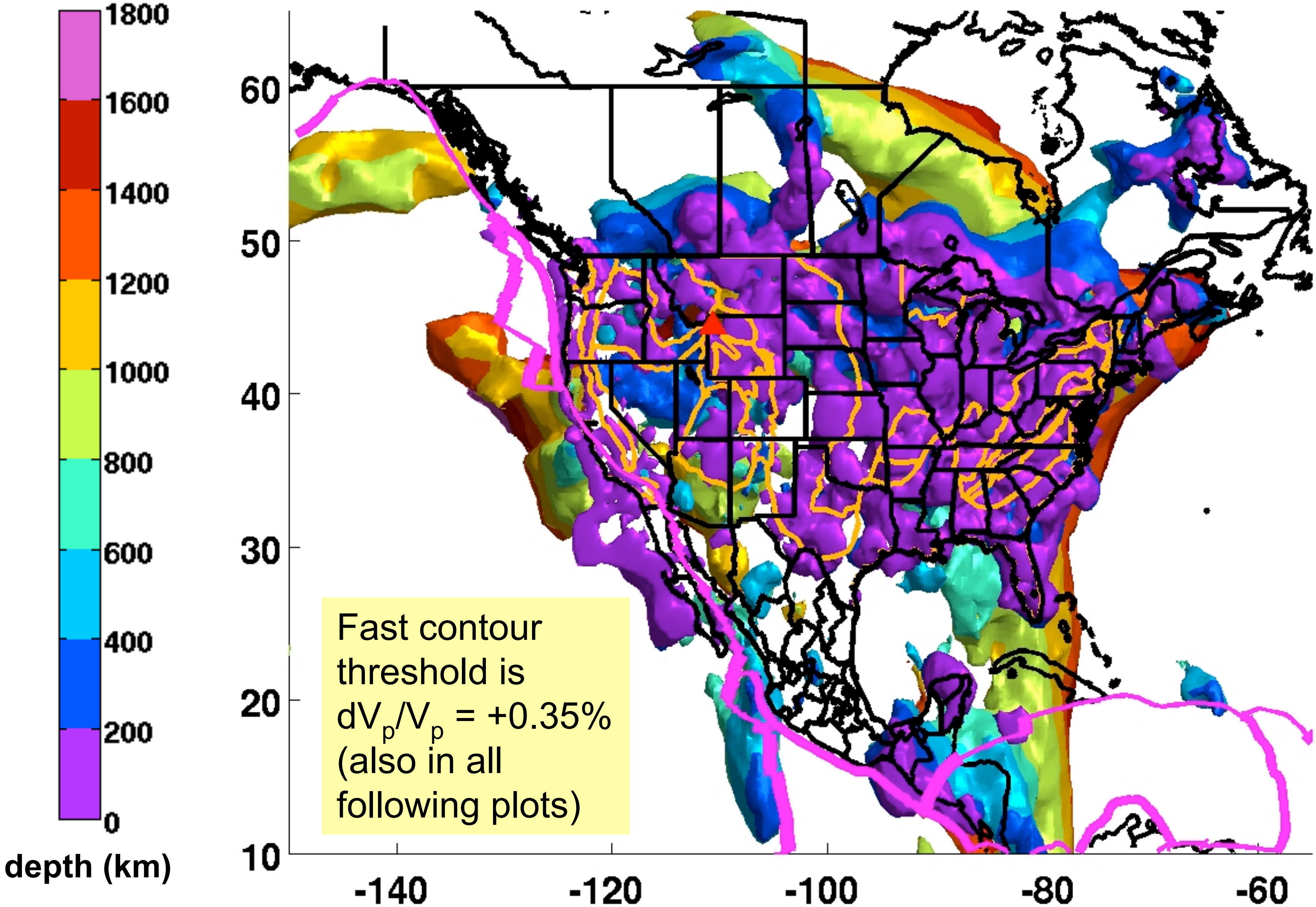


Fast contour threshold is $dV_p/V_p = +0.35\%$ (also in all following plots)

# Fast material below 300 km depth

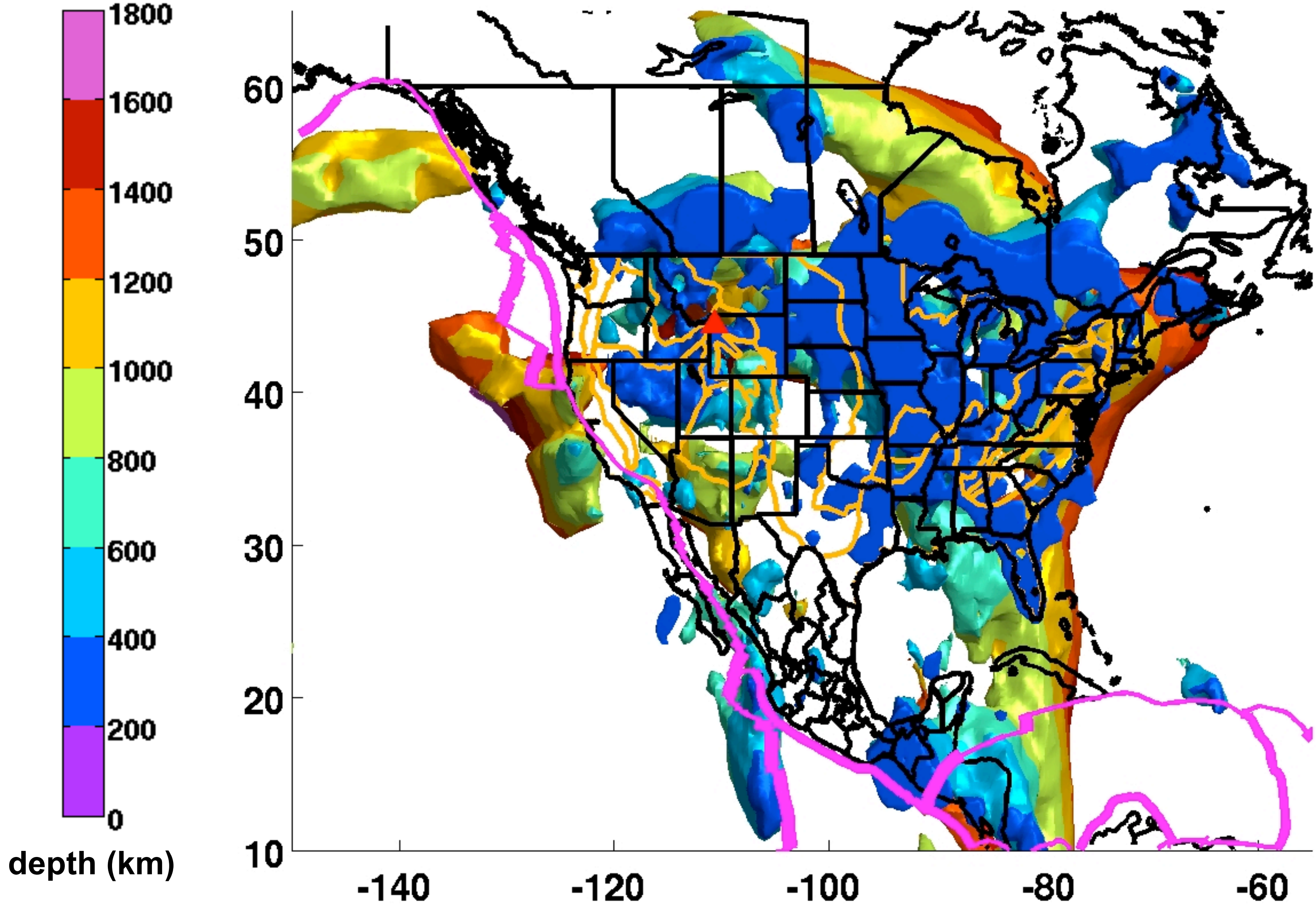

# Fast material below 700 km depth

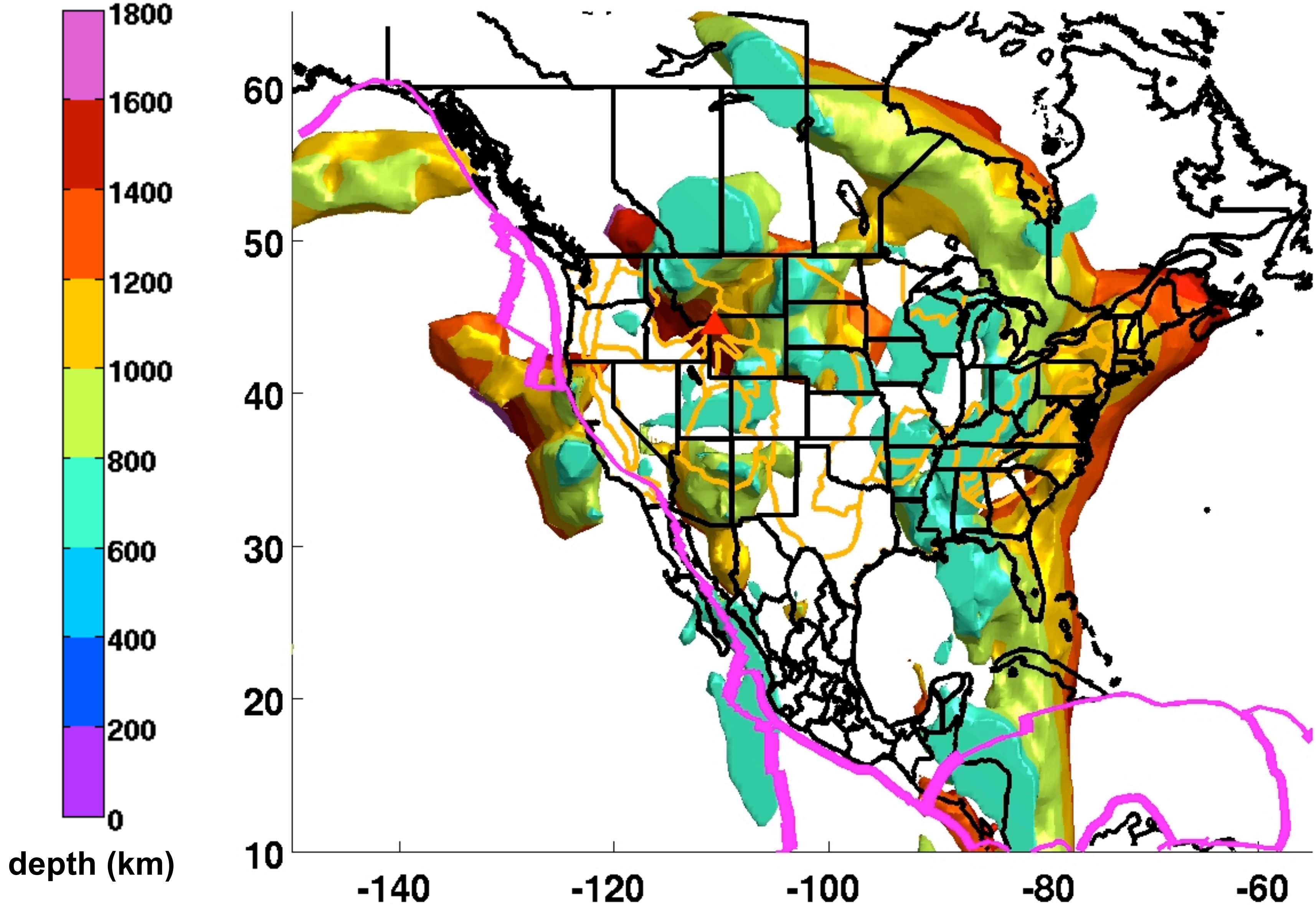

# All fast material (view from below)

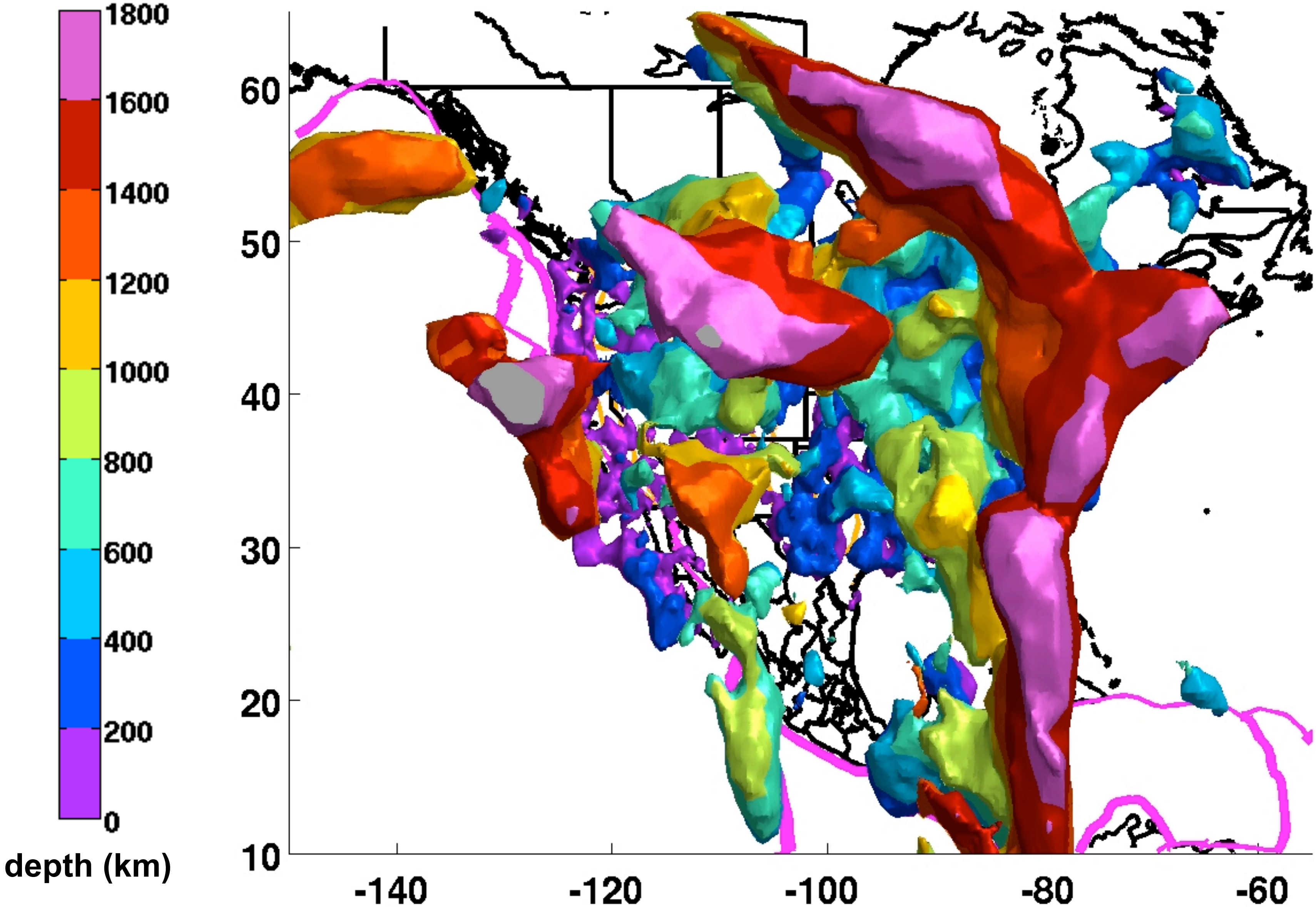

# Finite-frequency measurements

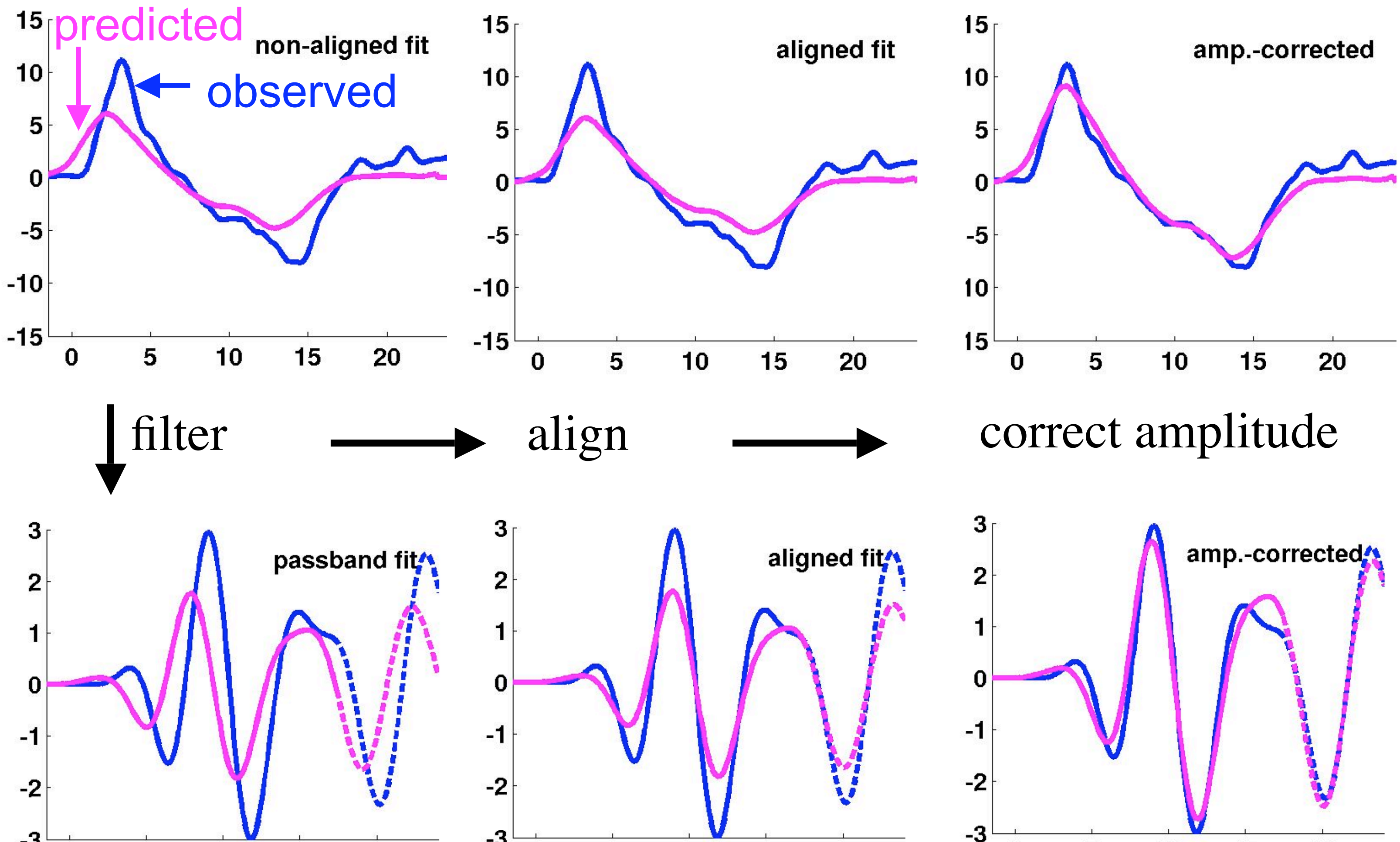


**⇒ traveltime anomaly**

**⇒ amplitude anomaly**

Sigloch & Nolet, GJI 2006

# Seismic waves sample the earth from surface to core

Seismogram: a time series recording of ground displacement, of a fixed point at the surface.

The seismology community collects (and shares) thousands of seismograms per big earthquake.

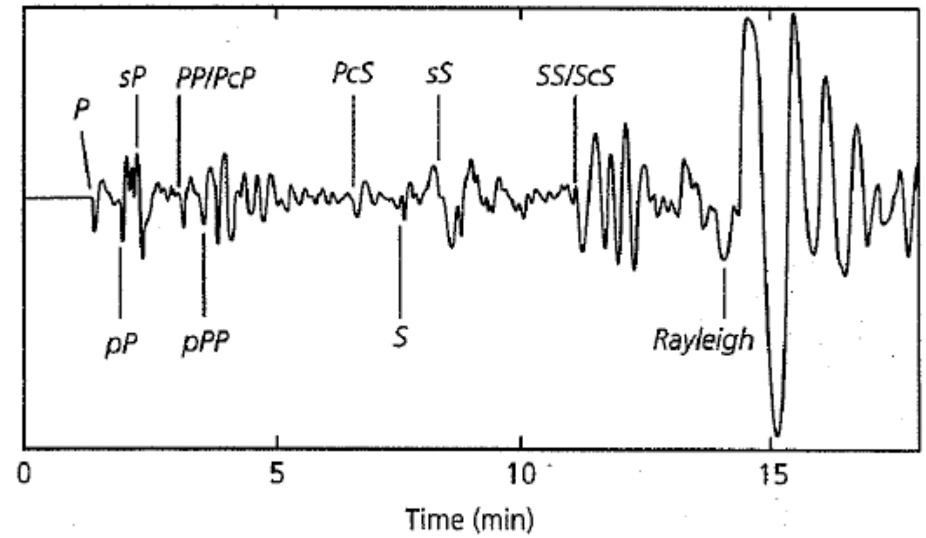


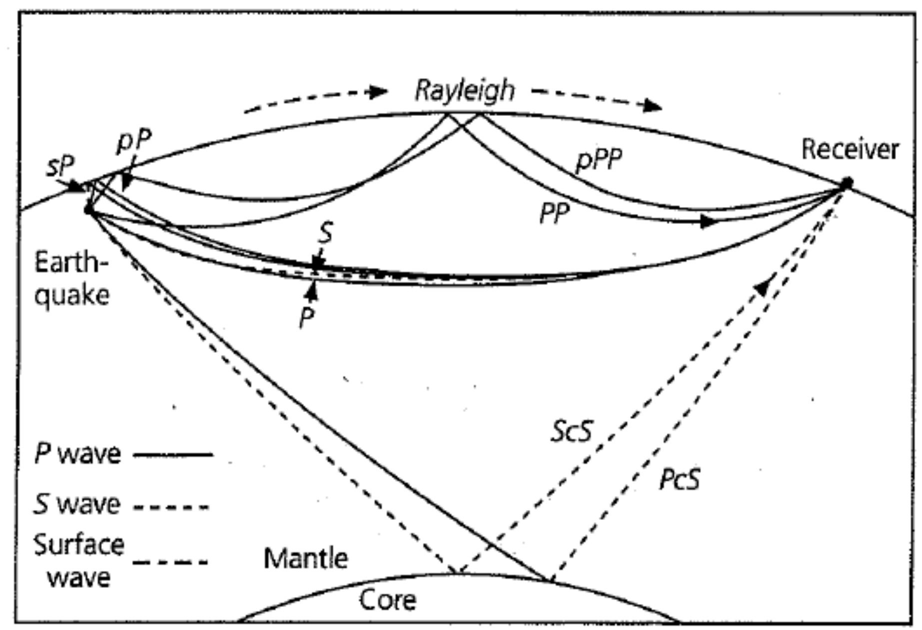

# Waves propagating in the spherical earth

- •Wave fields: simulations of wave propagation (showing a snapshot in time).
- •To first order, the earth is a layered medium, i.e. stratified by gravity.
- •Top: wavefronts from optical ray theory (approximative method). Bottom: full numerical solution of the seismic wave equation

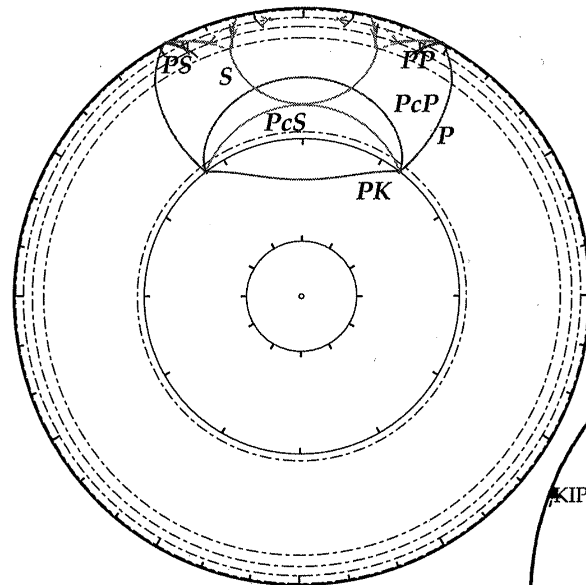


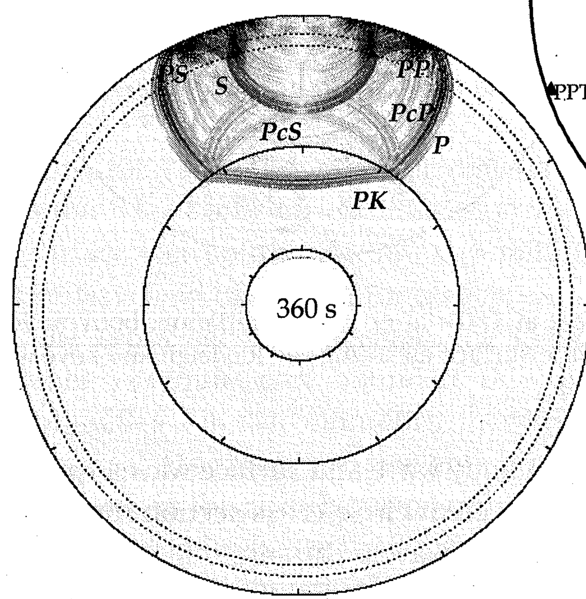


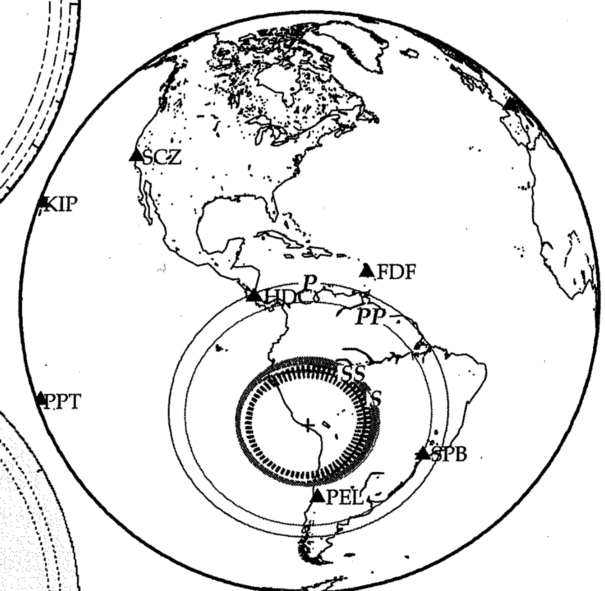


Global wavefronts, 360 sec after a large earthquake in Peru (from Kennett 2002).

# Causes of amplitude anomalies

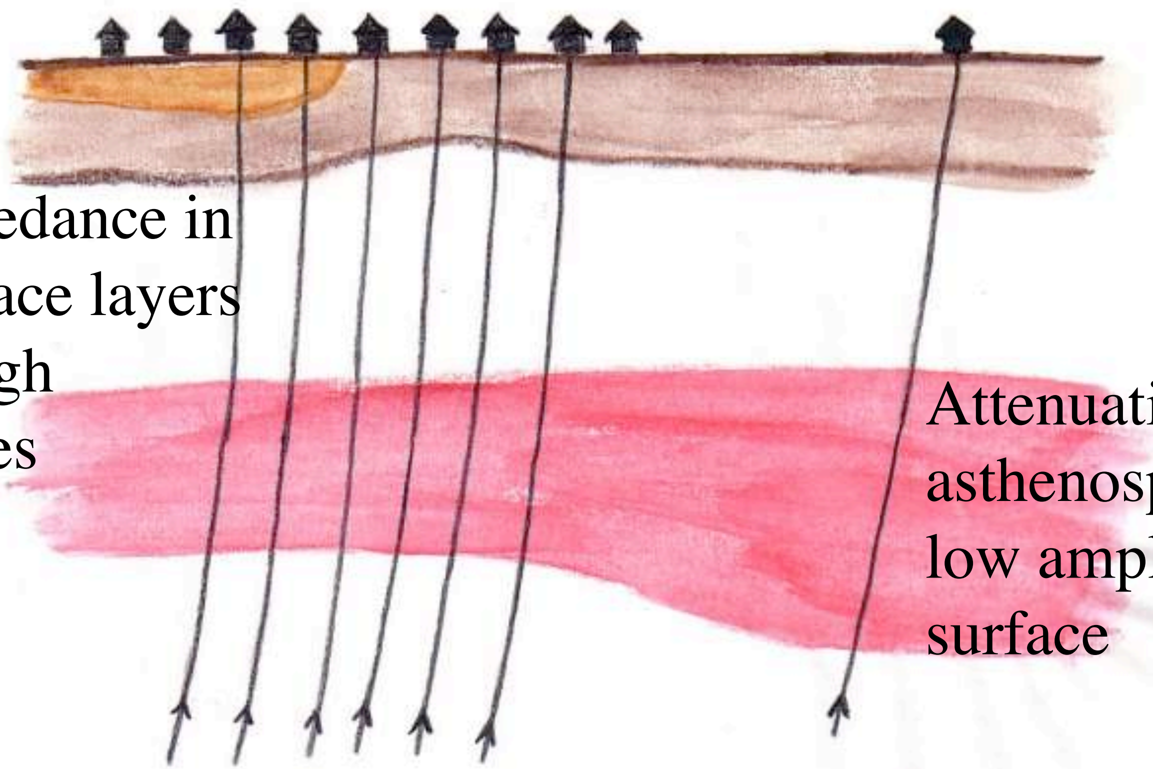

Low impedance in near-surface layers causes high amplitudes

Attenuation in the asthenosphere causes low amplitudes at the surface